

PROJECT ADMINISTRATION DATA SHEET

ORIGINAL REVISION NO. _____

Project No. E-16-668 R6102-OAO GTRC/~~OR~~ DATE 3 / 10 / 86

Project Director: Dr. L.W. Rehfield School/~~Lab~~ AE

Sponsor: NASA Langley Research Center Hampton, VA. 23665

Type Agreement: Grant NO. NAG-1-638

Award Period: From 2/12/86 To 2/11/87 (Performance) 2/11/87 (Reports)

Sponsor Amount:	<u>This Change</u>	<u>Total to Date</u>
Estimated: \$	<u>50,000</u>	\$ <u>50,000</u>
Funded: \$	<u>50,000</u>	\$ <u>50,000</u>

Cost Sharing Amount: \$ 5,496 Cost Sharing No: E-16-383 FG102-OAO

Title: Analysis, Design, And Elastic Tailoring Of Composite Rotor Blades

ADMINISTRATIVE DATA

OCA Contact R. Dennis Farmer x-4820

1) Sponsor Technical Contact:

2) Sponsor Admin/Contractual Matters:

Mark W. Nixon

John F. Royall

Army Aero. Research Group

Grants Officer

NASA Langley Research Center

NASA Langley Research Center

Mail Stop 226

Mail Stop 126

Hampton, VA. 23665

Hampton, VA. 23665

(804) 865-2866

(804) 865-3215

Defense Priority Rating: N/A

Military Security Classification: Unclassified

(or) Company/Industrial Proprietary: N/A

RESTRICTIONS

See Attached NASA Supplemental Information Sheet for Additional Requirements.

Travel: Foreign travel must have prior approval - Contact OCA in each case. Domestic travel requires sponsor approval where total will exceed greater of \$500 or 125% of approved proposal budget category.

Equipment: Title vests with Georgia Tech if less than \$1,000; Govt. Reserves the right to transfer title to itself for items costing \$1,000 or more, however, no equipment is proposed.

COMMENTS:



COPIES TO:

SPONSOR'S I. D. NO. 02.105.001.86.001

Project Director
 Research Administrative Network
 Research Property Management
 Accounting

Procurement/EES Supply Services
 Research Security Services
 Reports Coordinator (OCA)
 Research Communications (2)

GTRC
 Library
 Project File
 Other

SPONSORED PROJECT TERMINATION/CLOSEOUT SHEET

11-2
8/16/87

Date Sept 17, 1987

Project No. E-16-668

School/Lab AR

Includes Subproject No.(s) N/A

Project Director(s) Dr. L.W. Rehfield

GTRC / ~~SDC~~

Sponsor NASA Langley Research Center

Title Analysis, Design and Elastic Tailoring of Composite Rotor Blades
~~Analysis, Design and Elastic of Composite Rotor Blades~~

Effective Completion Date: 6/11/87

(Performance) 6/11/87

(Reports)

Grant/Contract Closeout Actions Remaining:

- None
- Final Invoice or Final Fiscal Report
- Closing Documents
- Final Report of Inventions Patent Questionnaire sent to P.I.
- Govt. Property Inventory & Related Certificate
- Classified Material Certificate
- Other _____

Continues Project No. _____

Continued by Project No. _____

COPIES TO:

- Project Director
- Research Administrative Network
- Research Property Management
- Accounting
- Procurement/GTRI Supply Services
- Research Security Services
- Report Director (OCA)
- Legal Services

- Library
- GTRC
- Research Communications (2)
- Project File
- Other _____

SEMIANNUAL STATUS REPORT
GRANT NO. NAG-1-638
GEORGIA TECH PROJECT E16-668

Lawrence W. Rehfield
Principal Investigator

Attached is a report entitled "Some Observations on the Behavior of the Langley Model Rotor Blade." This report was presented to Mr. Mark Nixon in person at the Langley Research Center on 24 July 1986. The report summarizes work completed in the first six-month period.

At this meeting, the decision was made to emphasize development of a multicell theory for the remainder of the grant period.



"SOME OBSERVATIONS ON THE BEHAVIOR
OF THE LANGLEY MODEL ROTOR BLADE"

Interim Report
Grant NAG-1-638
July 1986

Lawrence W. Rehfield and Ali R. Atilgan
Center for Rotary Wing Aircraft Technology
Georgia Institute of Technology
Atlanta, Georgia 30332

INTRODUCTION

In our statement of work for this grant, the first item is "support and coordinate with research underway at the Aerostructures Directorate" This interim report supports the design of the model rotor and the comparative study of coupled beam theory and the finite element analysis performed earlier at the Aerostructures Directorate by Robert Hodges and Mark Nixon.

Attention is focused upon two matters --- (1) an examination of the small discrepancies between twist angle predictions under pure torque and radial loading and (2) an assessment of nonclassical effects in bending behavior.

Our primary objective is understanding, particularly with regard to cause-effect relationships. Understanding, together with the simple, affordable nature of the coupled beam analysis, provides a sound basis for design.

STATIC APPLIED LOADING CASES

The three load cases considered by Hodges and Nixon have been considered here. The first case is bending due to lift and blade weight, the second is pure torque and the third is axial loading due to centrifugal force.

There is some inconsistency in the equations for the applied loading. In the present work, the coordinate X is taken from the blade root, which is radial station 5.23.

Bending Due to Lift and Blade Weight

The distributed loading is

$$q_z = 0.02222X - 0.0123 \text{ (lbs/in)} \quad (1)$$

The rotor model cross section appears in Figure 1. The coupled beam analysis of this loading case appears in Attachment 1.

Beam deflection results appear in Figure 2. Bernouli-Euler, the classical engineering beam theory, results are denoted by "BE." This model is overly stiff. Also presented are three shear deformation models, SD1, SD2 and SD3, and the finite element results.

The shear deformation model S1 is an approximation obtained by setting the coupling stiffness C_{25} and C_{36} to zero. This is the classical shear deformation model in the spirit of Timoshenko. Clearly it is overly stiff also. This direct transverse shear effect is small for a beam of this slenderness.

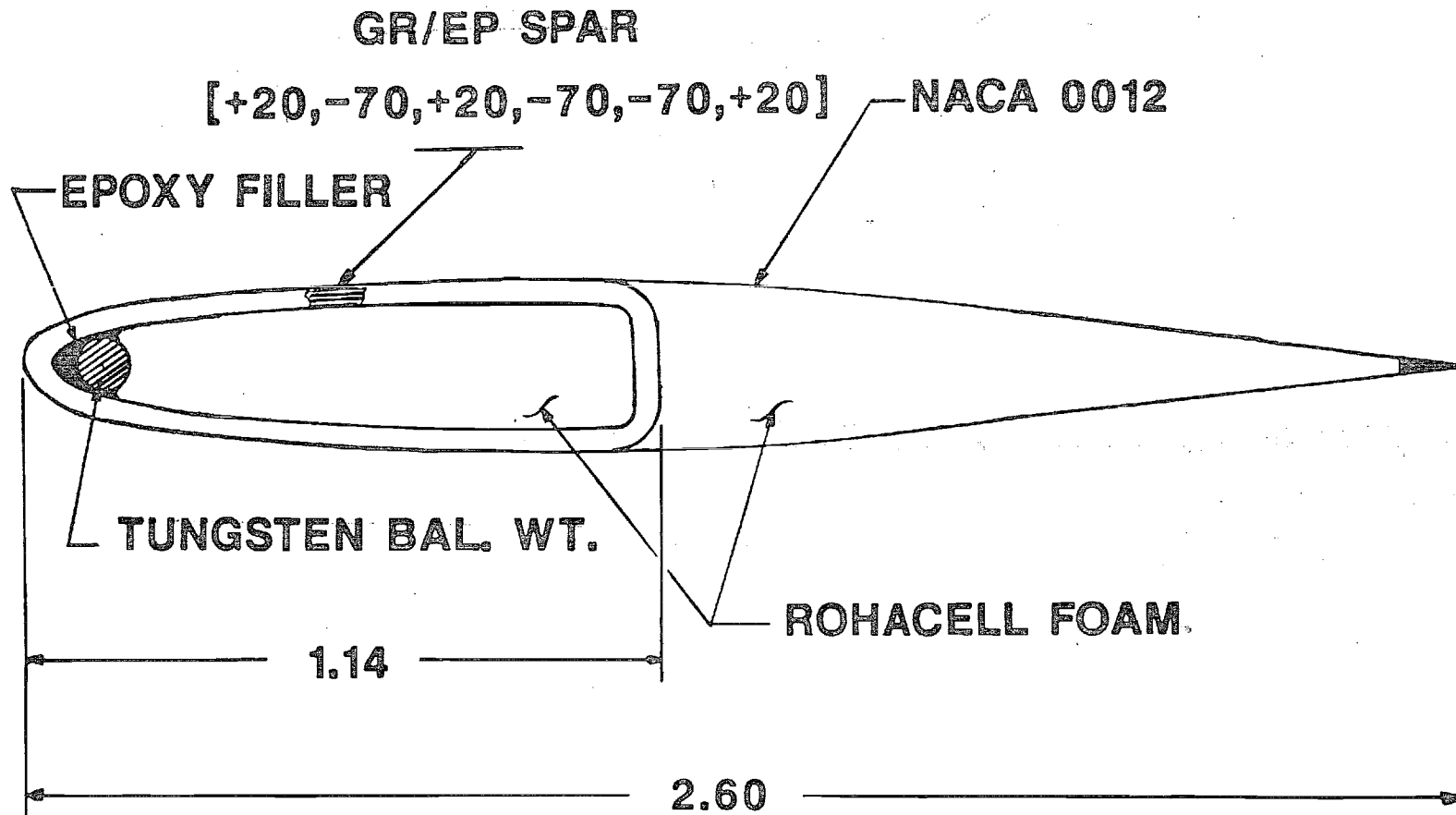
The complete theory, which includes all coupling effects, is denoted SD3. It provides good agreement with the finite element results.

The approximation denoted SD2 is obtained by neglecting completely the classical shear deformation effect accounted for in SD1 in favor of the coupling mechanism associated with C_{25} and C_{36} . This model, therefore, includes only deformations due to the transverse shear-bending coupling and the usual bending contribution. The magnitude of this new, unexplored form of elastic coupling is seen to be enormous by comparing SD2 and BE results. This is a finding of major importance in understanding the behavior.

The SD2 or SD3 models are required in this application in order to get sufficiently accurate predictions. This clearly excludes the earlier classical type theory of Mansfield and Sobey from practical use.

FIG. 1

MODEL ROTOR CROSS SECTION



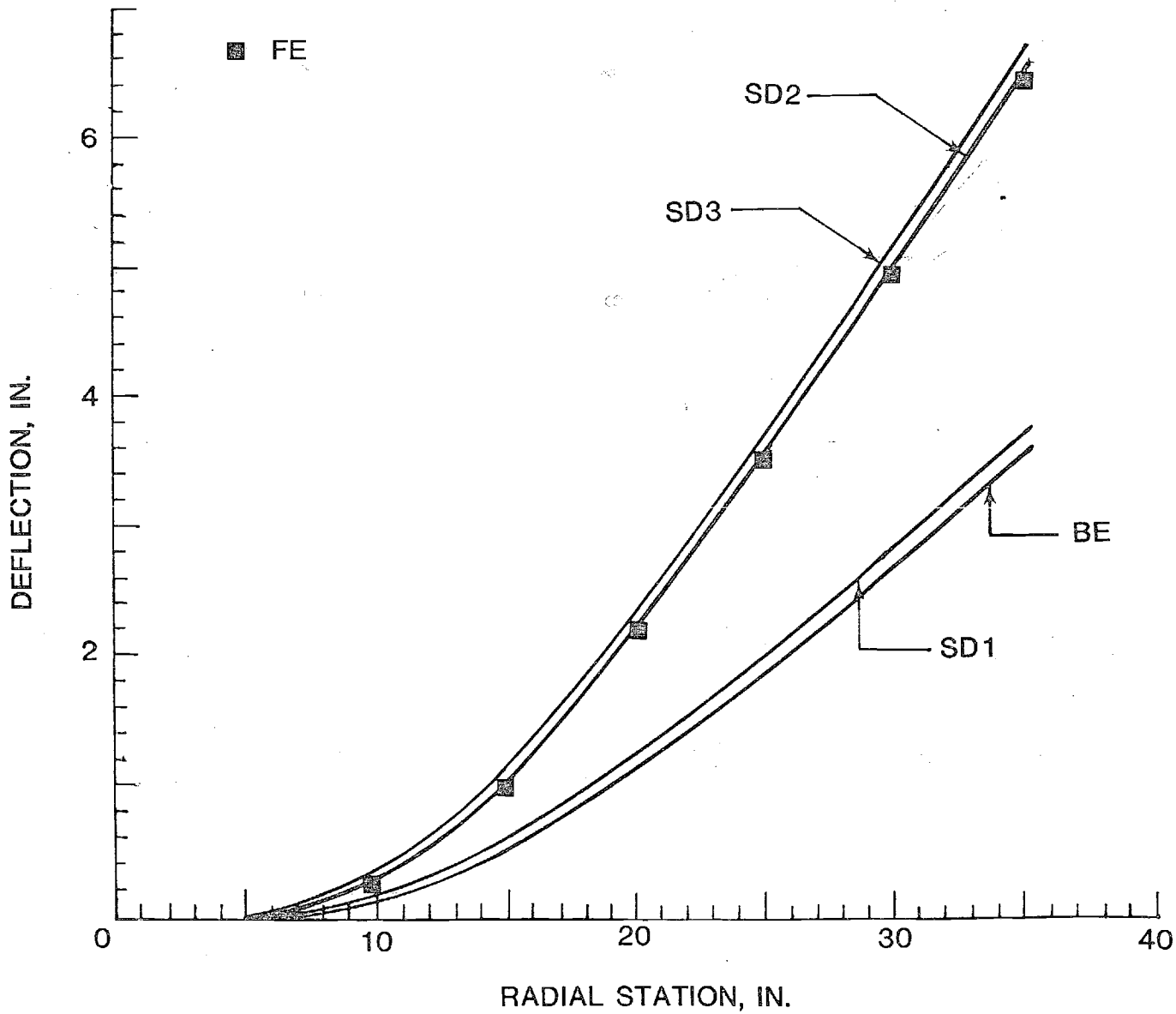


FIGURE 2
 BEAM DEFLECTION DUE TO
 LIFT AND BLADE WEIGHT

Pure Torque

Although there was generally good agreement for the torsion case in the Hodges-Nixon comparative study, the effect of torsion-related warping was not included. This effect has been included in the analysis presented in Attachment 2.

The classical St. Venant torsion theory result (without warping) is compared to the complete beam theory (CBT) and the finite element results in Figure 3. The CBT results, which differ from the classical (CL) only by the warping effect, are in excellent agreement with the finite element analysis. Restrained warping creates a boundary layer zone near the blade root that acts to stiffen the blade and reduce the angle of twist.

Axial Loading Due to Centrifugal Force

This case is of the utmost importance because extension-twist coupling is to be used to control blade stall. In the Hodges-Nixon comparative study, the classical St. Venant theory was utilized for the coupled beam analysis. The discrepancy between analytical predictions and the finite element analysis was the greatest for this case. Classical theory was too soft and it overestimated the twist angle, a condition that is not conservative in view of the stated purpose of the model demonstration.

As in the pure torsion case, the neglect of torsion-related warping is the reason for the discrepancy between coupled beam theory and the finite element analysis. A complete analysis of this loading case is given in Attachments 3 and 4. Attachment 3 contains the overall response analysis. The axial force distribution is

$$N = 913.83 - 7.875X - 0.75287X^2 \text{ (lb.)} \quad (2)$$

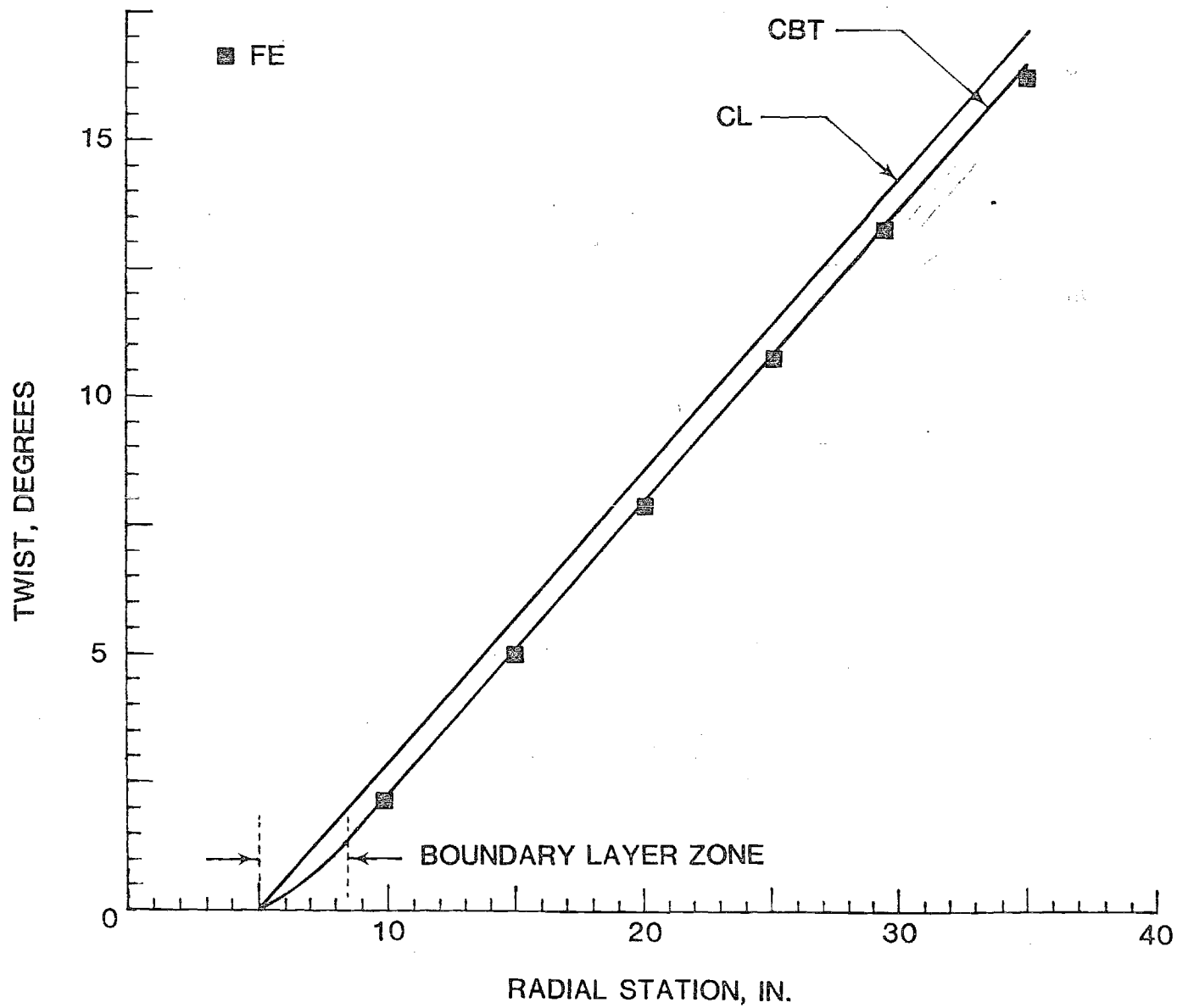


FIGURE 3

TWIST DUE TO APPLIED TORQUE

This expression differs from that quoted in the Hodges-Nixon work due to use of different coordinates.

The twist angle distribution appears in Figure 4. The use of CBT brings the beam theory results in very good agreement with the finite element analysis. The rate of twist distribution is given in Figure 5. Again, the agreement is very good.

Attachment 4 contains an analysis of the strain distributions for this loading case. The strain distributions are given in Figures 6 and 7. The results indicate that structural damage would be likely to occur at radial station 10 ($X \approx 5$) rather than at the root as predicted by classical theory.

WARPING ANALYSIS

A complete analysis of the effects of torsion-related warping appears in Attachment 5. Also included is a description of a simple warping model that is based upon a rectangular approximation for the cell. The equivalent rectangle is chosen to possess the same enclosed area. An assessment of this model suggests that it is adequate for the complete analysis.

The main difficulty in accounting for warping is determination of the warping function and the stiffness C_{77} . Both are accomplished readily with the approximate rectangular model.

CONCLUSIONS

In structures designed for extension-twist coupling, a high degree of bending-shear coupling is present which drastically causes the structure to be more flexible in bending. The impact of this effect on system performance must be assessed.

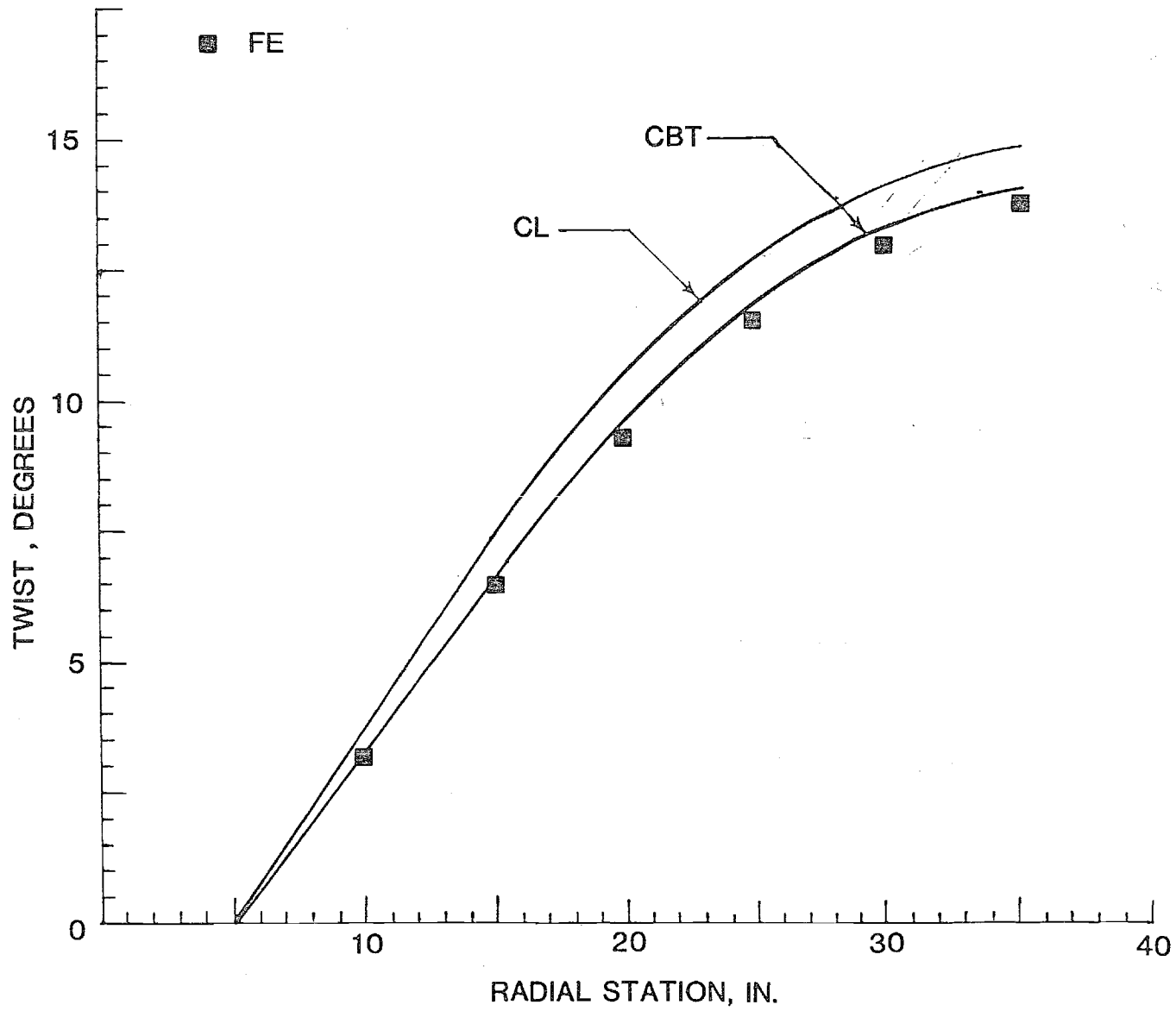


FIGURE 4

TWIST DUE TO CENTRIFUGAL TORQUE

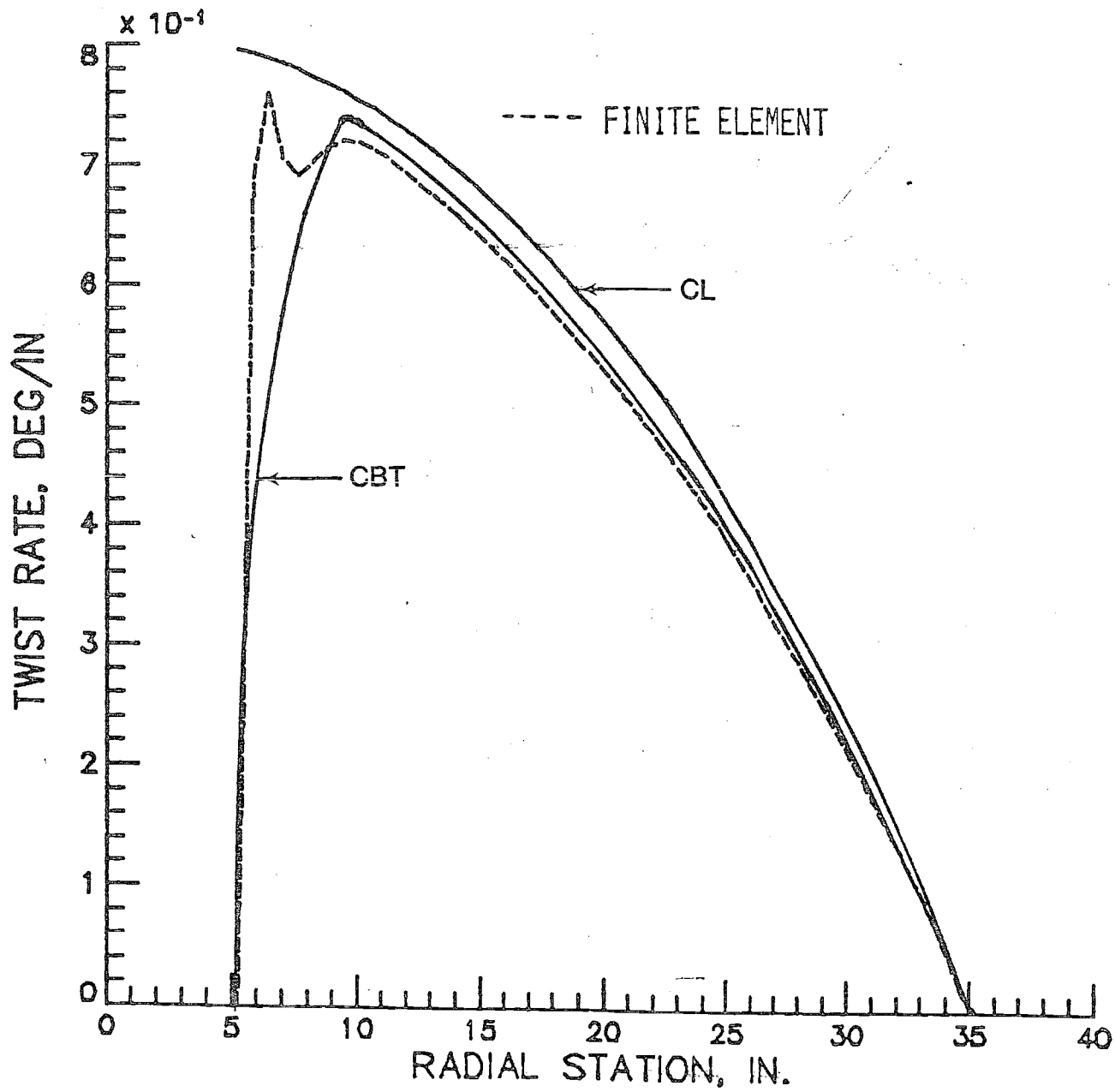


Figure 5. - Twist rate due to centrifugal force.

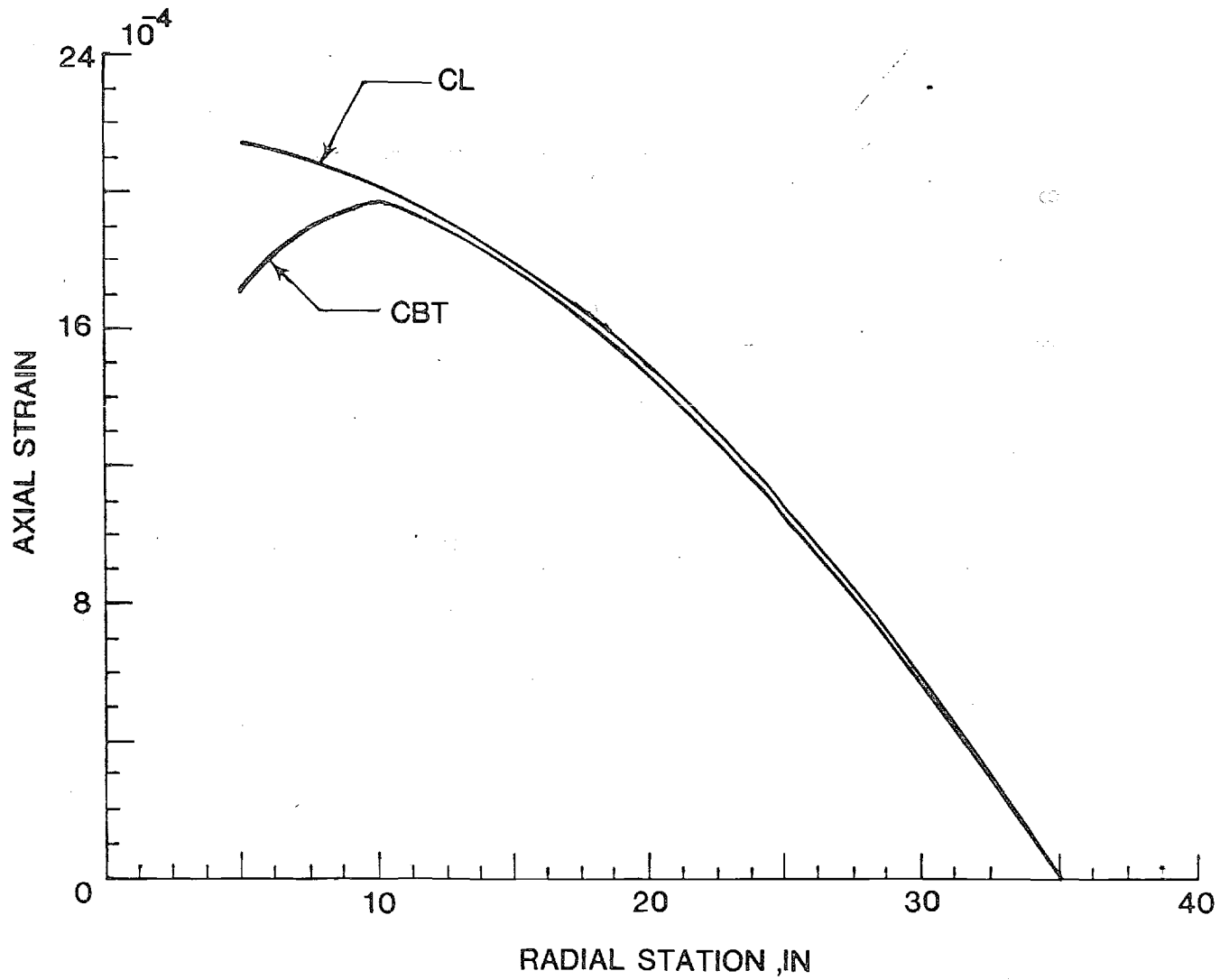


FIGURE 6

AXIAL STRAIN DUE TO CENTRIFUGAL FORCE

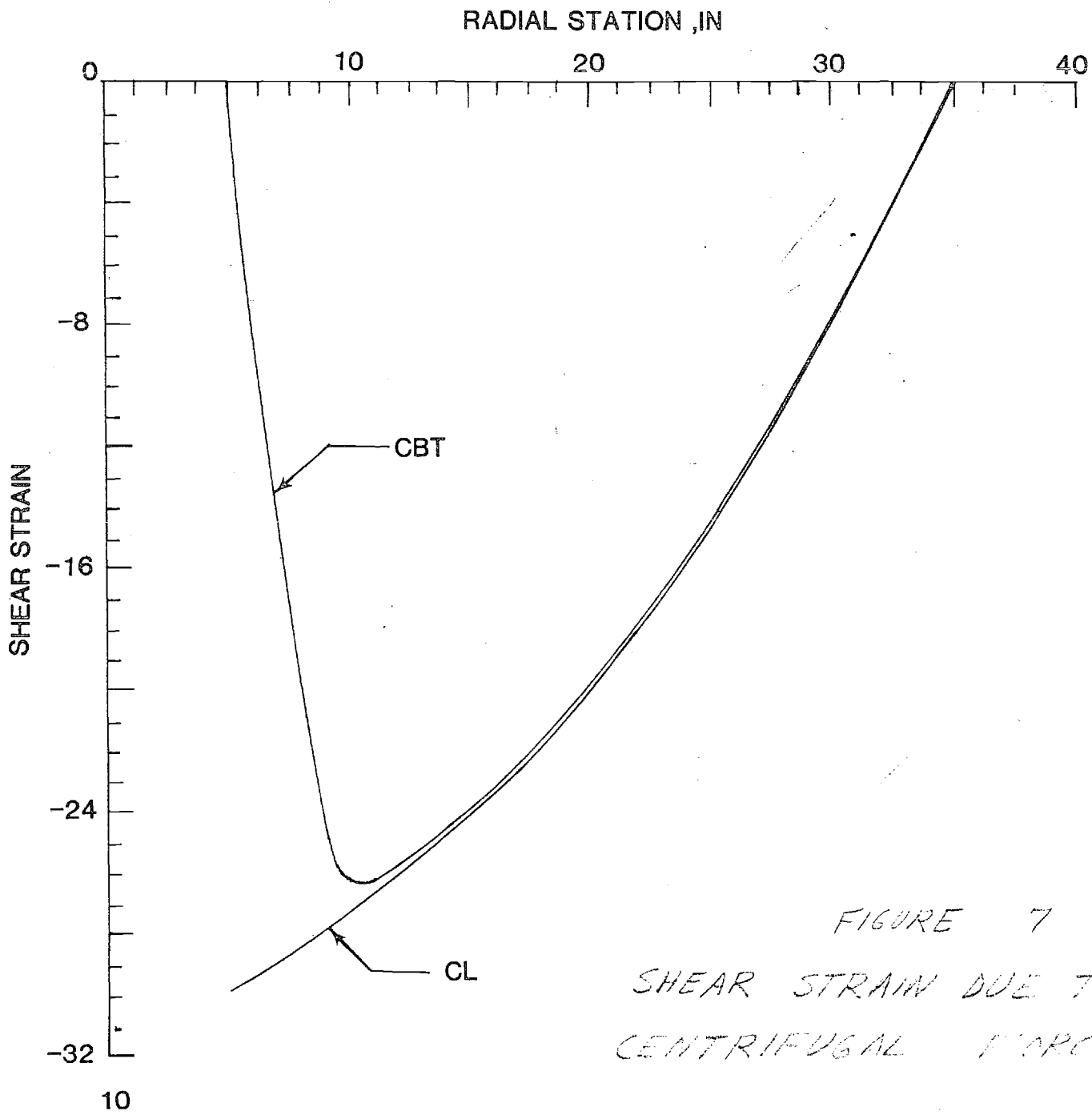


FIGURE 7
 SHEAR STRAIN DUE TO
 CENTRIFUGAL FORCE

Torsion-related warping is significant enough to warrant its inclusion in the beam analysis. A simple rectangular approximation may be used, which avoids the complexities associated with warping function and warping stiffness determination for sections similar to the D spar. With warping accounted for, the coupled beam theory is extremely accurate and easy to use.

ATTACHMENT 1

6 July 1986

COMPARISON OF COMPOSITE ROTOR BLADE MODELS :
CLASSICAL, CLASSICAL SHEAR DEFORMATION,
SHEAR DEFORMATION and AN MSC NASTRAN SHELL ELEMENT

A BENCH MARK CASE :

BEAM DEFLECTION DUE TO LIFT and BLADE WEIGHT

THEORY

The beam cross section rotation about the y axis is written in terms of beam compliance terms and applied loads

$$\beta_{y,x} = S_{25} Q_y + S_{55} M_y \quad (1)$$

The section rotation about the y axis is also defined in terms of the shear strain and the transverse displacement

$$\beta_y = \gamma_{xz} - W_{,x} \quad (2)$$

Derivation of equation (2) respect to x gives

$$\beta_{y,x} = \gamma_{xz,x} - W_{,xx} \quad (3)$$

The shear strain, γ_{xz} , can then be written in terms of beam compliance terms and applied loads

$$\gamma_{xz} = S_{33} Q_z + S_{36} M_z \quad (4)$$

Derivation of equation (4) respect to x yields

$$\gamma_{xz,xx} = S_{33} Q_{z,xx} + S_{36} M_{z,xx} \quad (5)$$

Substitution of equation (5) into equation (3) gives

$$\beta_{y,xx} = S_{33} Q_{z,xx} + S_{36} M_{z,xx} - W_{,xx} \quad (6)$$

and substitution $\beta_{y,xx}$ into equation (1) defines the deflection as

$$-W_{,xx} = S_{25} Q_y + S_{55} M_y - S_{33} Q_{z,xx} - S_{36} M_{z,xx} \quad (7)$$

In this case

$$Q_y = M_z = 0 \quad (8)$$

therefore equation (7) becomes

$$-W_{,xx} = S_{55} M_y - S_{33} Q_{z,xx} \quad (9)$$

Derivation of the shear, $Q_{z,xx}$, gives the load p

$$Q_{z,xx} = -p \quad (10)$$

so, equation (9)

$$-W_{,xx} = S_{55} M_y + S_{33} p \quad (11)$$

Shear Deformation Model

Rewrite equation (11)

$$-W_{,xx} = S_{55} M_y + S_{33} p$$

where

$$S_{55} = 1 / (C_{55} - C_{25}^2 / C_{22}) \quad (11a)$$

and

$$S_{33} = 1 / (C_{33} - C_{36}^2 / C_{66}) \quad (11b)$$

Classical Shear Deformation Model

In this model, it is presumed that

$$C_{25} = C_{36} = 0 \quad (12)$$

so, equations (11a) & (11b) become

$$S_{55} = 1 / C_{55} \quad (13a)$$

$$S_{33} = 1 / C_{33} \quad (13b)$$

thus equation (11) is refined as

$$-W_{,xx} = \frac{M_y}{C_{55}} + \frac{P}{C_{33}} \quad (14)$$

Classical Model

In the classical model, it is assumed that shear strain is negligible; therefore equation (8)

$$\beta_{y,x} = -W_{,xx} \quad (15)$$

and using equation (8)

The deflection is found to be as

$$-W_{,xx} = \frac{M_y}{C_{55}} \quad (16)$$

APPLICATION

The load, p , due to lift and blade weight can be written in terms of x as

$$p = 0.02222x - 0.0123 \quad [\text{lbs/in}] \quad (17)$$

Integrating once gives the shear

$$Q_z = -0.01111x^2 + 0.0123x + C_1 \quad (18)$$

B.C. is

$$Q_z \Big|_{x=30} = 0 \quad (19)$$

so

$$Q_z = -0.01111x^2 + 0.0133x + 9.631 \quad [\text{lbs}] \quad (20)$$

Integrating again gives the moment

$$M_y = -0.003704x^3 + 0.00615x^2 + 2.631x + C_2 \quad (21)$$

B.C. is

$$M_y \Big|_{x=30} = 0 \quad (22)$$

so

$$M_y = -0.003704x^3 + 0.00615x^2 + 2.631x - 194.5 \quad [\text{lb-in}] \quad (23)$$

Come back to equation (11); integrating twice with using boundary conditions which are

$$W_{,x} \Big|_{x=0} = 0 \quad (24a)$$

$$W \Big|_{x=0} = 0 \quad (24b)$$

gives the deflection function as follows

$$W = Ax^5 - Bx^4 - (C+D)x^3 + (E+F)x^2 \quad (25)$$

Shear Deformation Model

In this model, the coefficients in equation (25) are defined as

$$A = S_{55} \cdot A^* \quad (26 \text{ a})$$

$$B = S_{55} \cdot B^* \quad \text{b)}$$

$$C = S_{55} \cdot C^* \quad \text{c)}$$

$$D = S_{33} \cdot D^* \quad \text{d)}$$

$$E = S_{55} \cdot E^* \quad \text{e)}$$

$$F = S_{33} \cdot F^* \quad \text{f)}$$

where

$$A^* = 0.003704 / 20 \quad ; \quad B^* = 0.00615 / 20 \quad , \quad C^* = 9.631 / 6$$

$$D^* = 0.02222 / 6 \quad \quad E^* = 194.5 / 2 \quad ; \quad F^* = 0.0123 / 2$$

Classical Shear Deformation Model

In this model, the coefficients in equation (25) are defined as

$$A = A^* / C_{55} \quad (27 \text{ a})$$

$$B = B^* / C_{55} \quad \text{b)}$$

$$C = C^* / C_{55} \quad \text{c)}$$

$$D = D^* / C_{33} \quad \text{d)}$$

$$E = E^* / C_{55} \quad \text{e)}$$

$$F = F^* / C_{33} \quad \text{f)}$$

The coefficients, A, B, C, D, E and F are seen in table 2 and 3 for shear deformation and classical shear deformation model respectively.

Classical Model

In this model, the coefficients A, B, C, E are the same coefficients as defined in equation (27); D and F variable.

RESULTS

$C_{33} = 0.3071 E5$	$C_{25} = 0.3147 E5$
$C_{55} = 0.1337 E5$	$C_{36} = -0.3147 E5$
$S_{33} = 0.4561 E-4$	$S_{55} = 0.1356 E-3$

Table.1. Beam stiffnesses and beam compliance terms

$A = 2.5113 E-8$	$C = 0.2176 E-3$
$B = 6.9495 E-8$	$E = 13.1871 E-3$
$D = 0.1689 E-8$	$F = 28.8251 E-8$

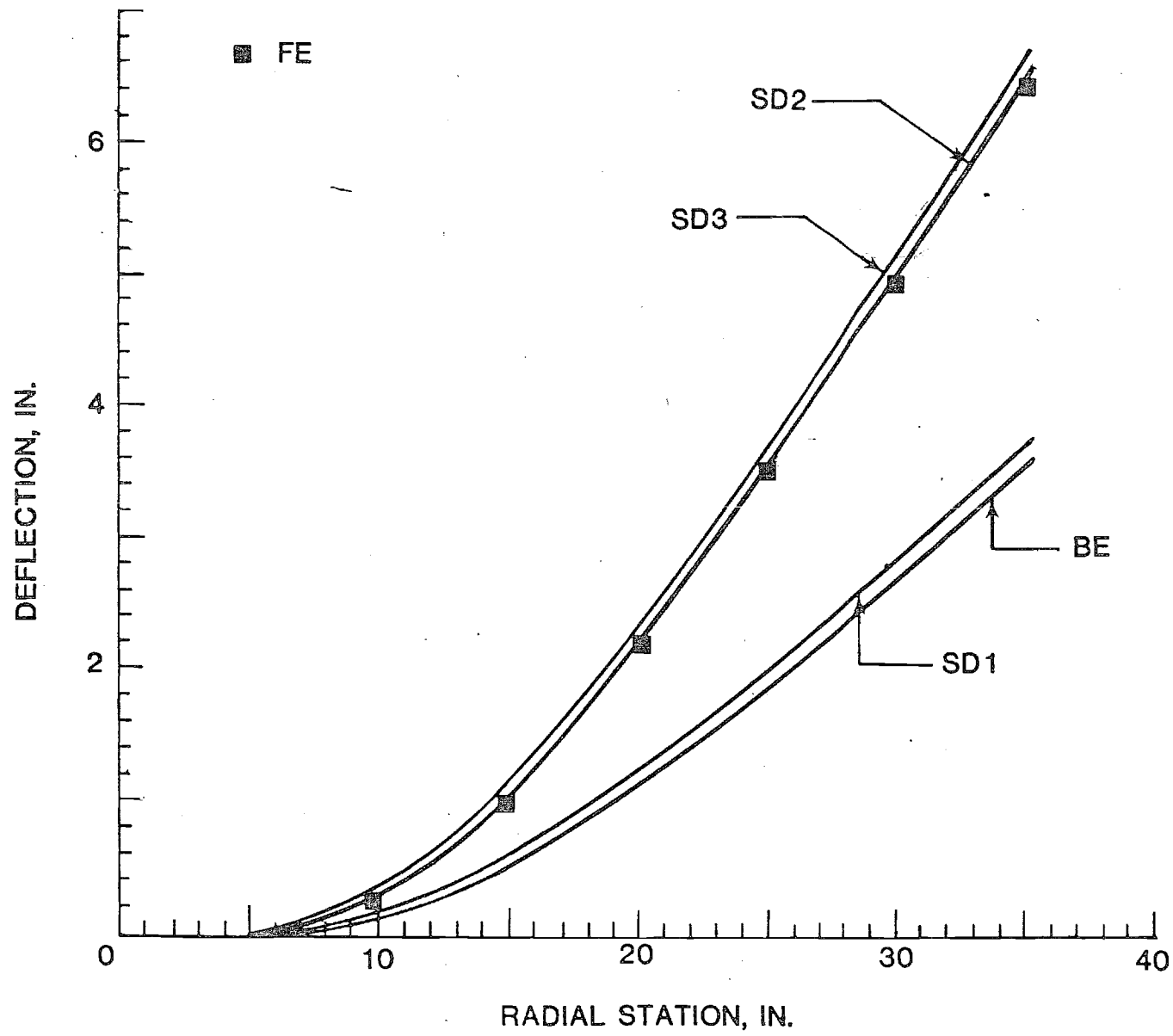
Table.2. Coefficients for shear deformation model

$A = 1.3852 E-8$	$C = 0.1201 E-3$
$B = 3.8532 E-8$	$E = 7.2738 E-3$
$D = 0.1206 E-8$	$F = 20.0261 E-8$

Table.3. Coefficients for classical shear deformation model

	RADIAL STATION	5.23	10.23	15.23	20.23	25.23	30.23	35.23	[IN]
(SD3)	COMPLETE SHEAR DEFORMATION	0	0.3025	1.0961	2.2483	3.6035	5.0603	6.6018	
FE	FINITE ELEMENT	0	0.30	1.09	2.23	3.58	4.99	6.53	
(SD1)	CLASSICAL SHEAR DEFORMATION	0	0.1669	0.6083	1.2445	1.9870	2.7902	3.6405	[IN]
(BE)	CLASSICAL	0	0.1658	0.6063	1.2395	1.9762	2.7875	3.6297	
(SD2)	NON-CLASSICAL SHEAR DEFORMATION	0	0.3014	1.0949	2.2471	3.5828	5.0572	6.5448	

Table 4. Beam deflection due to blade weight and lift for different models used.

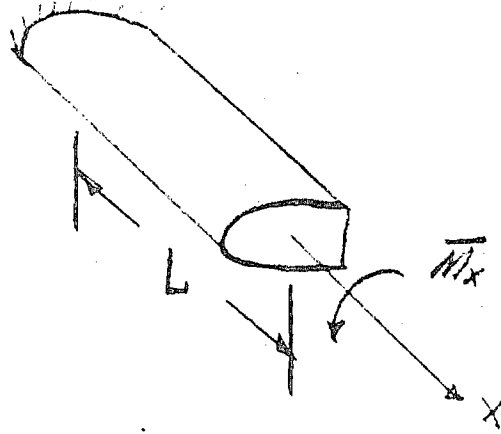


ATTACHMENT 2

10 July 8

Warping Effects in the Rotor Blade Model

Consider the root fixed and a tip torque applied.



$$\bar{M}_x = C_T \varphi_{,x} - C_{TT} \varphi_{,xxx} \quad (1)$$

where

$$C_T = C_{44} - \frac{(C_{14})^2}{C_{11}} \quad (2)$$

At $x=0$: $\varphi = 0$, $\varphi_{,x}(0) = 0$ (No warping)

The classical St. Venant solution is

$$\varphi_{cl} = \frac{\bar{M}_x}{C_T} x \quad (3)$$

With restrained warping, the solution is found from

$$\varphi = \varphi_{cl} + \varphi' \quad (4)$$

$$C_T \varphi' - C_{TT} \varphi'_{,xx} = C_1 \quad \text{or}$$

$$\varphi'_{,xx} - p^2 \varphi' = -\frac{C_1}{C_{TT}} \quad (5)$$

Assume that only the decaying root need be used so that

$$\phi' = C_2 e^{-px} + C_1' \quad (8)$$

Therefore

$$\phi = C_2 e^{-px} + C_1' + \frac{\bar{M}_x x}{C_T} \quad (9)$$

$$\phi' = -pC_2 e^{-px} + \frac{\bar{M}_x}{C_T}$$

$$C_2 = \frac{\bar{M}_x}{pC_T} \quad (10)$$

$$C_1' = -C_2 \quad (11)$$

so

$$\phi = \frac{\bar{M}_x}{C_T} \left[\frac{1}{p} (e^{-px} - 1) + x \right] \quad (12)$$

Tip Deflection:

$$\phi(L) = \frac{\bar{M}_x}{C_T} \left(L - \frac{1}{p} \right) = \frac{\phi(L)}{C_T} \left(1 - \frac{1}{Lp} \right)$$

where

$$p^2 = \frac{C_T}{C_{TT}} \quad (14)$$

CALCULATION OF TIP DEFLECTION

$$C_T = C_{44} - \frac{C_{14}^2}{C_{11}}$$

$$C_T = 0.49925 \text{ E4} \quad [\text{lb-in}^2]$$

$$p^2 = \frac{C_T}{C_{77}}$$

$$C_{77} = 0.06645 \text{ E5} \quad [\text{lb-in}^4]$$

$$p^2 = 0.751317 \quad [1/\text{in}^2]$$

$$p = 0.867 \quad [1/\text{in}]$$

$$\frac{\varphi_w(L)}{\varphi_{cl}(L)} = 1 - \frac{1}{L \cdot p}$$

$$\frac{\varphi_w(L)}{\varphi_{cl}(L)} = 0.96$$

$$\varphi_{cl}(L) = \frac{\overline{M}_x \cdot L}{C_T} \cdot (57.3)$$

$$\varphi_{cl}(L) = 17.19$$

$$\varphi_w(L) = 16.50$$

ATTACHMENT 3

10 July 1986

TWIST UNDER EXTENSION
- Rotor Blade Model -

The axial force distribution is

$$N = 913.83 - 7.875x - 0.75287x^2 \quad (1a)$$

or

$$N = N_0 - N_1x - N_2x^2 \quad (1b)$$

We desired the twist with no torque applied.

$$\begin{aligned} (M_x)_{\text{Total}} &= C_{11}U_{,x} + C_{44}\varphi_{,x} - C_{77}\varphi_{,xxx} \\ &= 0 \end{aligned} \quad (2)$$

$$N = C_{11}U_{,x} + C_{14}\varphi_{,x} \quad (3)$$

Eliminate $U_{,x}$ in (2)

$$U_{,x} = \frac{C_{77}}{C_{14}}\varphi_{,xxx} - \frac{C_{44}}{C_{14}}\varphi_{,x} \quad (4)$$

Substitute the above into (3)

$$N = \frac{C_{11}}{C_{14}} (C_{77}\varphi_{,xxx} - C_T\varphi_{,x}) \quad (5)$$

where

$$C_T = C_{44} - \frac{C_{14}^2}{C_{11}}$$

Therefore

$$\psi_{,xxx} - p^2 \psi_{,x} = \frac{C_{14}}{C_{11}C_{77}} (N_0 - N_1 x - N_2 x^2) \quad (6)$$

where

$$p^2 = \frac{C_T}{C_{77}}$$

let say

$$K = \frac{C_{14}}{C_{11}C_{77}}$$

and integrate (6)

$$\psi_{,xx} - p^2 \psi = K \left(N_0 x - \frac{N_1}{2} x^2 - \frac{N_2}{3} x^3 + k_1 \right) \quad (7)$$

Particular solution

$$\psi_p = a_0 + a_1 x + a_2 x^2 + a_3 x^3 \quad (8)$$

so

$$2a_2 + 6a_3 x - p^2(a_0 + a_1 x + a_2 x^2 + a_3 x^3) = K \left(N_0 x - \frac{N_1}{2} x^2 - \frac{N_2}{3} x^3 + k_1 \right)$$

$$6a_3 - p^2 a_1 = K N_0$$

$$-p^2 a_2 = -\frac{K N_1}{2}$$

(9)

$$-p^2 a_3 = -\frac{K N_2}{3}$$

$$-p^2 a_0 + 2a_2 = K k_1$$

The solution of system (9) is

$$a_0 = \frac{K}{p^2} \left(\frac{N_1}{p^2} - k_1 \right) \quad (10a)$$

$$a_1 = \frac{K}{p^2} \left(\frac{2N_2}{p^2} - N_0 \right) \quad b)$$

$$a_2 = \frac{KN_1}{2p^2} \quad c)$$

$$a_3 = \frac{KN_2}{3p^2} \quad d)$$

Therefore the particular solution is

$$\varphi_p = \frac{K}{p^2} \left\{ \left(\frac{N_1}{p^2} - k_1 \right) + \left(\frac{2N_2}{p^2} - N_0 \right) x + \frac{N_1}{2} x^2 + \frac{N_2}{3} x^3 \right\} \quad (11)$$

The form of the solution is

$$\varphi = C_2 e^{-px} + \frac{K}{p^2} \left\{ \left(\frac{N_1}{p^2} - k_1 \right) + \left(\frac{2N_2}{p^2} - N_0 \right) x + \frac{N_1}{2} x^2 + \frac{N_2}{3} x^3 \right\} \quad (12)$$

Boundary conditions

$$\varphi_{,2}(0) = 0 \quad (13a)$$

$$-pC_2 + \frac{K}{p^2} \left\{ \frac{2N_2}{p^2} - N_0 \right\} = 0 \quad b)$$

$$\varphi(0) = 0 \quad (14a)$$

$$C_2 + \frac{K}{p^2} \left(\frac{N_1}{p^2} - k_1 \right) = 0 \quad b)$$

thus

$$C_2 = \frac{1}{p} \cdot \frac{K}{p^2} \left\{ \frac{2N_2}{p^2} - N_0 \right\} \quad (15a)$$

and

$$k_1 = \frac{1}{p} \left\{ \frac{2N_2}{p^2} - N_0 \right\} - \frac{N_1}{p^2} \quad c)$$

Therefore

$$\phi = \frac{K}{P^2} \left\{ \left(\frac{2N_2}{P^2} - N_0 \right) \left[\frac{1}{P} \left(e^{-Px} - 1 \right) + x \right] + \frac{2N_1}{P^2} + \frac{N_1}{2} x^2 + \frac{N_2}{3} x^3 \right\}$$

CALCULATION OF TIP DEFLECTION

$$\phi_{cl}(L) \Big|_{L=30} = 14.9$$

$$\phi_{\omega}(L) \Big|_{L=30} = 13.927$$

(Circle approach is used to determine C_{77})

$$\phi_{\omega}(L) \Big|_{L=30} = 13.998$$

(Rectangular approach is used to find C_{77})

$$\phi_{FEM}(L) \Big|_{L=30} \approx 14.$$

ATTACHMENT 4

15 July 1986

STRAINS UNDER EXTENSION

CLASSICAL THEORY

The axial force distribution is

$$N = N_0 - N_1 x - N_2 x^2 \quad (1)$$

If one desires the twist with no torque applied the following will be written:

$$(M_x)_{\text{Total}} = C_{14} U_{,x} + C_{44} \varphi_{,x} = 0 \quad (2)$$

so,

$$U_{,x} = - \frac{C_{44}}{C_{14}} \varphi_{,x} \quad (3)$$

The axial strain is

$$(E_{xx})_{cl} = U_{,x} + y\beta_{z,x} + z\beta_{y,x} \quad (4)$$

and

$$M_y = M_z = 0 \quad (5)$$

therefore

$$\beta_{y,x} = - \frac{C_{25}}{C_{55}} \gamma_{xy} \quad (6)$$

and

$$\beta_{z,x} = - \frac{C_{36}}{C_{66}} \gamma_{xz} \quad (7)$$

also

$$\gamma_{xy} = S_{22} Q_y + S_{25} M_y \quad (8)$$

and

$$\gamma_{xz} = S_{33} Q_z + S_{36} M_z \quad (9)$$

Since there is no shear force

$$Q_y = Q_z = 0 \quad (10)$$

With the aid of the equations (5) and (10)

$$\gamma_{xy} = \gamma_{xz} = 0 \quad (11)$$

therefore from equations (6) and (7)

$$\beta_{y,x} = \beta_{z,x} = 0 \quad (12)$$

thus equation (4) becomes

$$(E_{xx})_{CL} = U_{,x} \quad (13)$$

Using equation (3)

$$(E_{xx})_{CL} = -\frac{C_{44}}{C_{14}} \varphi_{,x} \quad (14)$$

From compliance relationship

$$\varphi_{,x} = S_{14} N \quad (15)$$

Using equation (1) and (15) into (14) yields

$$(\epsilon_{xx})_{CL} = \frac{C_{44}}{C_{14}} S_{14} (N_0 - N_1 x - N_2 x^2) \quad (16)$$

The membrane shear strain is

$$(\gamma_{xs})_{CL} = \gamma_{xy} \frac{dy}{ds} + \gamma_{xz} \frac{dz}{ds} + \frac{2A_e}{C} \varphi_{,x} \quad (17)$$

Since γ_{xy} and γ_{xz} is zero (equation 11)

$$(\gamma_{xs})_{CL} = \frac{2A_e}{C} \varphi_{,x} \quad (18)$$

or

$$(\gamma_{xs})_{CL} = \frac{2A_e}{C} S_{14} \cdot (N_0 - N_1 x - N_2 x^2) \quad (19)$$

COMPLETE BEAM THEORY

The form of the total torque is

$$(M_x) = C_{14} U_{,x} + C_{44} \varphi_{,x} - C_{77} \varphi_{,xxx} = 0 \quad (20)$$

If one eliminates $U_{,x}$ in above

$$U_{,x} = \frac{C_{77}}{C_{14}} \varphi_{,xxx} - \frac{C_{44}}{C_{14}} \varphi_{,x} \quad (21)$$

The axial strain is

$$(\epsilon_{xx})_{CBT} = \frac{C_{77}}{C_{14}} \varphi_{,xxx} - \frac{C_{44}}{C_{14}} \varphi_{,x} + \psi \varphi_{,xx} \quad (22)$$

The closed form solution of φ is

$$\varphi = \frac{K}{P^2} \left\{ \left(\frac{2N_2}{P^2} - N_0 \right) \left[\frac{1}{P} (e^{-px} - 1) + x \right] + \frac{2N_1}{P^2} + \frac{N_1}{2} x^2 + \frac{N_2}{3} x^3 \right\} \quad (23)$$

so,

$$\varphi_{,x} = \frac{K}{P^2} \left\{ \left(\frac{2N_2}{P^2} - N_0 \right) (1 - e^{-px}) + N_1 x + N_2 x^2 \right\} \quad (24)$$

$$\varphi_{,xx} = \frac{K}{P^2} \left\{ \left(\frac{2N_2}{P^2} - N_0 \right) P e^{-px} + N_1 + 2N_2 x \right\} \quad (25)$$

$$\varphi_{,xxx} = \frac{K}{P^2} \left\{ \left(\frac{2N_2}{P^2} - N_0 \right) (-P^2 e^{-px}) + 2N_2 \right\} \quad (26)$$

Substitution of $\varphi_{,x}$, $\varphi_{,xx}$, $\varphi_{,xxx}$ into equation (22) gives

$$\begin{aligned} (E_{xx})_{CBT} &= \frac{C_{77}}{C_{14}} \frac{K}{P^2} \left[\left(\frac{2N_2}{P^2} - N_0 \right) (-P^2 e^{-px}) + 2N_2 \right] \\ &\quad - \frac{C_{44}}{C_{14}} \frac{K}{P^2} \left[\left(\frac{2N_2}{P^2} - N_0 \right) (1 - e^{-px}) + N_1 x + N_2 x^2 \right] \\ &\quad + \Psi_m \frac{K}{P^2} \left[\left(\frac{2N_2}{P^2} - N_0 \right) (P e^{-px}) + N_1 + 2N_2 x \right] \end{aligned} \quad (27)$$

where Ψ_m is the max value of warping function, which is

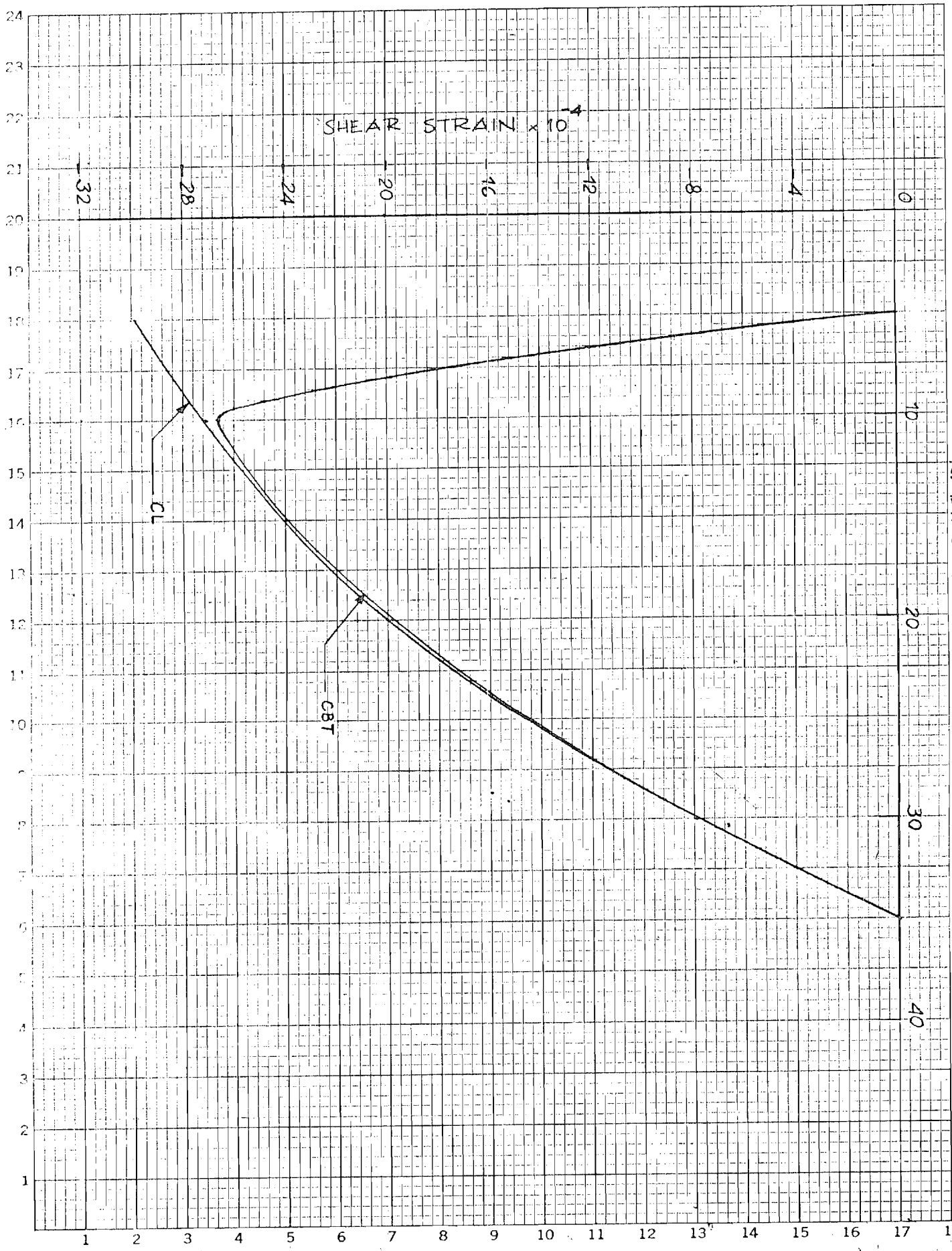
$$\Psi_m = -0.0464 \quad [IN^2] \quad (28)$$

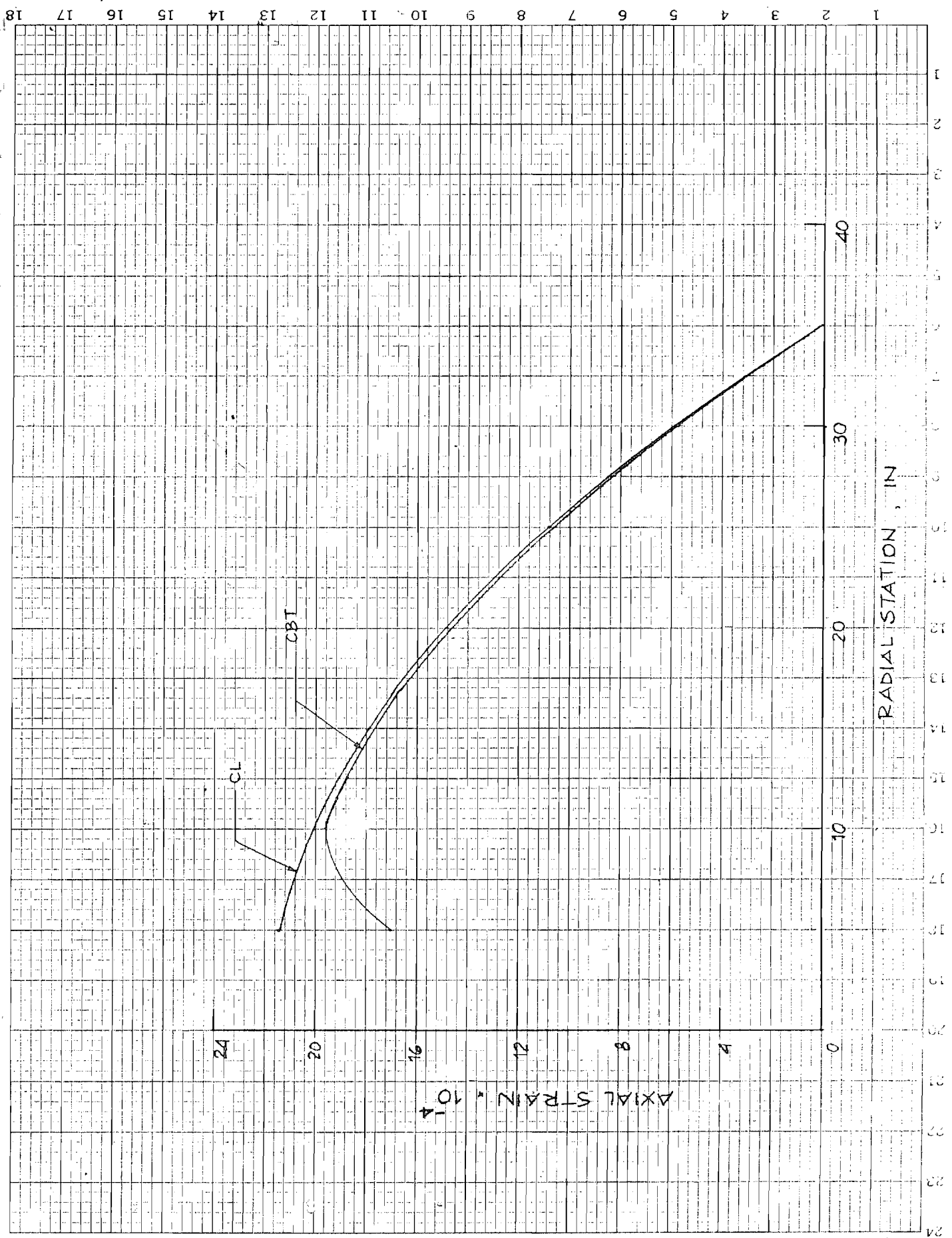
The membrane shear strain is

$$(\delta_{XS})_{\text{CBT}} = \frac{2Ae}{C} \cdot \psi_{,x} \quad (29)$$

or

$$(\delta_{XS})_{\text{CBT}} = \frac{2Ae}{C} \cdot \frac{K}{P^2} \left\{ \left(\frac{2N_2}{P^2} - N_0 \right) (1 - e^{-Px}) + N_1 x + N_2 x^2 \right\} \quad (30)$$





ATTACHMENT 5

14 July 1986

WARPING EFFECTS ON ROTOR BLADE MODELS

THE TORSION RELATED WARPING FUNCTION

The torsion related warping function, ψ , is defined as

$$\psi(s) = \frac{2A_e}{c} s - 2w(s) \quad (1)$$

where A_e is the enclosed area of the cross section, c is the circumference and

$$w(s) = \frac{1}{2} \int_0^s r_n ds \quad (2)$$

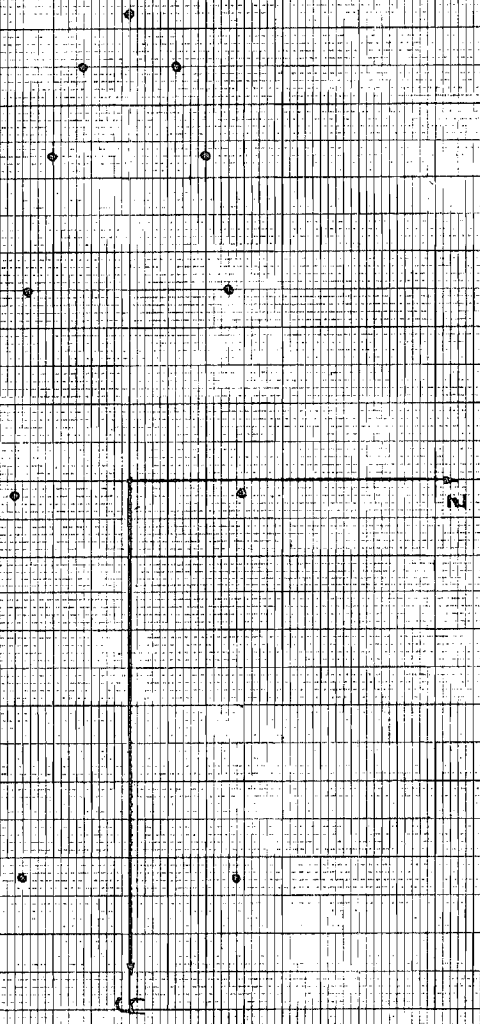
which is the sectorial area swept out as s increases

D spar cross sections

Co-ordinates of the D spar undertaken is shown in Fig. 1. In order to calculate the warping function, one of the co-ordinate, say z , has to be found the function of the other one, y ; to do so, the curve fitting method may be used. This analysis is summarized in Appendix I.

An other quick and useful approach to find the warping function is to consider the D spar as two regions: one of them is rectangular the other one is a part of a circle. This approach is shown in Fig. 2.

Fig. 1
Coordinates of the D spar



The radius of the circle considered is found to be as

$$R = \frac{H^2 + L^2}{2H} \quad (3)$$

To find the enclosed area the following method is used:

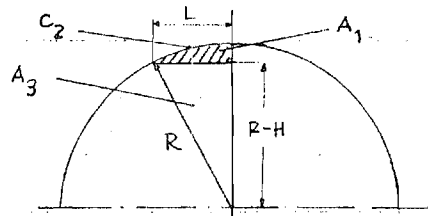


Fig.3.

The total area, $A_1 + A_3$, is

$$A_1 + A_3 = \frac{R^2}{2} \arcsin \frac{L}{R} \quad (4)$$

and A_3 is

$$A_3 = (R-H) \cdot \frac{L}{2} \quad (5)$$

therefore the area wanted, A_1 , is

$$A_1 = \frac{R^2}{2} \arcsin \frac{L}{R} - (R-H) \cdot \frac{L}{2} \quad (6)$$

The area of the rectangular region, A_2 , is

$$A_2 = L' \cdot H \quad (7)$$

thus, the total enclosed area of the D spar is

$$A_e = 2(A_1 + A_2) \quad (8a)$$

or

$$A_e = 2 \left[L'H + \frac{R^2}{2} \arcsin \frac{L}{R} - (R-H) \frac{L}{2} \right] \quad (8b)$$

The circumference of the circular part region, c_2 , is

$$c_2 = R \arcsin \frac{L}{R} \quad (9)$$

The circumference of the rectangular region, c_1 , is

$$c_1 = H + L' \quad (10)$$

then the total circumference of the D spar, c , is

$$c = 2(c_1 + c_2) \quad (11a)$$

or

$$c = 2 \left(L' + H + R \arcsin \frac{L}{R} \right) \quad (11b)$$

Therefore $\frac{2A_e}{c}$, let say

$$B = \frac{2A_e}{c} \quad (12)$$

so

$$B = \frac{L'H + \frac{R^2}{2} \arcsin \frac{L}{R} - (R-H) \frac{L}{2}}{L' + H + R \arcsin \frac{L}{R}} \quad (13)$$

Now, the warping function can be rewritten as

$$\psi(s) = Bs - 2w(s) \quad (14)$$

Since the main purpose is to find the warping stiffness, C_{77} , which is calculated by using a line integral :

$$C_{77} = \oint K_{11} \cdot \Psi^2 ds \quad (15)$$

and, now, let consider the lines shown in Fig2. are made out of different materials; therefore equation (15) becomes (using symmetry)

$$\frac{1}{2} C_{77} = \int_0^H K_{11}^{(1)} \Psi_1^2 ds + \int_H^{L'+H} K_{11}^{(2)} \Psi_2^2 ds + \int_{L'+H}^{c/2} K_{11}^{(3)} \Psi_3^2 ds \quad (16)$$

where

$$\Psi_1 = Bs - 2\omega_1(s) \quad 0 \leq s \leq H \quad (17)$$

$$\Psi_2 = Bs - 2\omega_2(s) \quad H \leq s \leq L'+H \quad (18)$$

$$\Psi_3 = Bs - 2\omega_3(s) \quad L'+H \leq s \leq \frac{c}{2} \quad (19)$$

so, we reduced the problem which is to find the sectorial areas swept out for each region.

For line 1

$$\Gamma_n = L' \quad (20)$$

so

$$2\omega_1(s) = \int_0^s L' ds \quad (21)$$

then

$$2\omega_1(s) = L's \quad 0 \leq s \leq H \quad (22)$$

For line 2

$$\Gamma_n = H \quad (23)$$

so

$$2\omega_2(s) = L'H + \int_0^s H ds \quad (24)$$

then

$$2\omega_2(s) = L'H + Hs \quad H \leq s \leq L'+H \quad (25)$$

For line 3, we have to find the shaded area, A' , as function of s . The form of A' is found by subtracting the area below the shaded area from the area of the circular part. One obtains the A' as

$$A' = \frac{1}{2} \left[R s - (R-H) R \sin \frac{s}{R} \right] \quad (26)$$

therefore

$$2w_3(s) = 2L'H + R s - (R-H) R \sin \frac{s}{R} \quad L'+H \leq s \leq \frac{c}{2} \quad (27)$$

Using equations (17) and (22) gives ψ_1 ,

$$\psi_1(s) = (B-L')s \quad 0 \leq s \leq H \quad (28)$$

Equations (18) and (25) gives ψ_2 ,

$$\psi_2(s) = (B-H)s - L'H \quad H \leq s \leq L'+H \quad (29)$$

and equations (19) and (27) gives ψ_3 ,

$$\psi_3(s) = (B-R)s + (R-H)R \sin \frac{s}{R} - 2L'H \quad L'+H \leq s \leq \frac{c}{2} \quad (30)$$

Equation (16) can be written as

$$C_{77} = 2 \left(K_{11}^{(1)} I_1 + K_{11}^{(2)} I_2 + K_{11}^{(3)} I_3 \right) \quad (31)$$

where

$$I_1 = \int_0^H [(B-L')s]^2 ds \quad (32a)$$

$$I_1 = \int_0^H (B-L')^2 s^2 ds = K_{11}^{(1)} \frac{(B-L')^2}{3} s^3 \Big|_0^H \quad (32b)$$

or

$$I_1 = \frac{(B-L')^2}{3} H^3 \quad (33)$$

and

$$I_2 = \int_H^{L'+H} [(B-H)s - L'H]^2 ds \quad (34a)$$

$$I_2 = \int_H^{L'+H} [(B-H)^2 s^2 - 2(B-H)L'Hs + L'^2 H^2] ds \quad (34b)$$

$$= \left[\frac{(B-H)^2}{3} s^3 - (B-H)L'Hs^2 + L'^2 H^2 s \right] \Big|_H^{L'+H}$$

so

$$I_2 = \left\{ \frac{(B-H)^2}{3} L' (L'^2 + 3L'H + 3H^2) - (B-H)L'^2 H(L'+2H) + L'^3 H^2 \right\} \quad (35)$$

and

$$I_3 = \int_{L'+H}^{c/2} \left[(B-R)s + (R-H)R \sin \frac{s}{R} - 2L'H \right]^2 ds \quad (36a)$$

$$I_3 = \int_{L'+H}^{c/2} \left[(B-R)^2 s^2 + (R-H)^2 R^2 \sin^2 \frac{s}{R} + 4L'^2 H^2 + 2(B-R)(R-H)R s \sin \frac{s}{R} - 4(R-H)RL'H \sin \frac{s}{R} - 4(B-R)L'Hs \right] ds \quad (36b)$$

$$I_3 = \left[\frac{(B-R)^2}{3} s^3 + (R-H)^2 R^2 \left(\frac{1}{2} s - \frac{R}{4} \sin \frac{2s}{R} \right) + 4L'^2 H'^2 s \right. \\ \left. + 2(B-R)(R-H)R \left(R^2 \sin \frac{s}{R} - s R \cos \frac{s}{R} \right) \right. \\ \left. - 4(R-H)RL'H \left(-R \cos \frac{s}{R} \right) - 2(B-R)L'Hs^2 \right] \Bigg|_{L'+H}^{c/2} \quad (36c)$$

$$I_3 = \left\{ \frac{(B-R)^2}{3} \left[\frac{c^3}{8} - (L'+H)^3 \right] + (R-H)^2 R^2 \left\{ \frac{1}{2} \left(\frac{c}{2} - L'-H \right) - \frac{R}{4} \left[\sin \frac{c}{R} - \sin \frac{2(L'+H)}{R} \right] \right. \right. \\ \left. \left. + 4L'^2 H'^2 \left(\frac{c}{2} - L'-H \right) \right. \right. \\ \left. \left. + 2(B-R)(R-H)R \left[R^2 \left(\sin \frac{c}{2R} - \sin \frac{L'+H}{R} \right) - \left[\frac{c}{2} R \cos \frac{c}{2R} - (L'+H)R \cos \frac{L'+H}{R} \right] \right. \right. \right. \\ \left. \left. \left. + 4(R-H)RL'H \left(R \cos \frac{c}{2R} - R \cos \frac{L'+H}{R} \right) - 2(B-R)L'H \left[\frac{c^2}{4} - (L'+H)^2 \right] \right\} \right\} \quad (36d)$$

so we know I_1 (equation (33)), I_2 (equation (35)) and I_3 (equation (37)).

If the D spar is made out of the same material

$$K_{11}^{(1)} = K_{11}^{(2)} = K_{11}^{(3)} = K_{11} \quad (38)$$

then

$$C_{77} = 2K_{11} (I_1 + I_2 + I_3) \quad (39)$$

The Equivalent Rectangular Area Approach

Let consider a rectangular cross section which has the same enclosed area as the D spar.

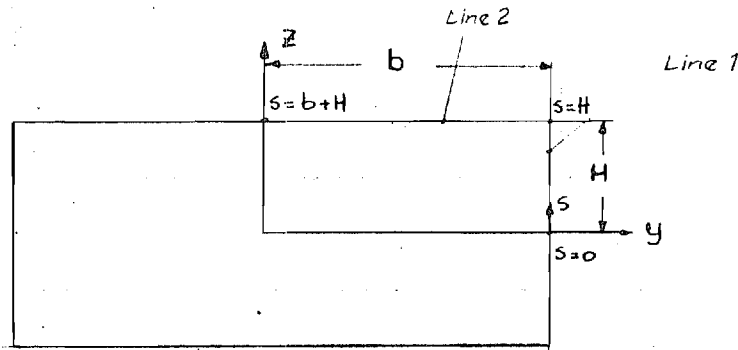


Fig. 4.

It is presumed that the rectangular has the same width, H , as the D spar; therefore

$$(A_e)_{D \text{ spar}} = 4bH \quad (40a)$$

or

$$b = \frac{(A_e)_{D \text{ spar}}}{4H} \quad (40b)$$

so, the circumference of the rectangular cross section is

$$(C)_{\text{rec}} = 4(b+H) \quad (41)$$

then the ratio of $\frac{2A_e}{C}$, B' ,

$$B' = \frac{2bH}{b+H} \quad (42)$$

The form of the warping function, Ψ_R , is

$$\Psi_R = B's - 2w(s) \quad (43)$$

We will follow the same procedure as what we have done for D spar case. Let say, Line 1 and Line 2 are made out of different materials. Using symmetry gives

$$C_{77}^R = 4 \left\{ \int_0^H K_{11}^{(1)} \Psi_{R1}^2 ds + \int_H^{b+H} K_{11}^{(2)} \Psi_{R2}^2 ds \right\} \quad (44)$$

where

$$\Psi_{R1} = B's - 2w_1(s) \quad 0 \leq s \leq H \quad (45)$$

$$\Psi_{R2} = B's - 2w_2(s) \quad H \leq s \leq b+H \quad (46)$$

For Line 1

$$r_n = b \quad (47a)$$

so

$$2w_1(s) = \int_0^s b ds \quad b) \quad (47b)$$

$$2w_1(s) = bs \quad 0 \leq s \leq H \quad (48)$$

For Line 2

$$r_n = H \quad (49a)$$

so

$$2w_2(s) = bH + \int_0^s H ds \quad b) \quad (49b)$$

$$2w_2(s) = bH + Hs \quad H \leq s \leq H+b \quad (50)$$

Using equations (45) and (48) gives

$$\Psi_{R1} = (B' - b)s \quad 0 \leq s \leq H \quad (51)$$

Equations (46) and (50) gives

$$\Psi_{R2} = (B' - H)s - bH \quad H \leq s \leq b+H \quad (52)$$

Equation (44) can be rewritten as

$$C_{77}^R = 4 \left(K_{11}^{(1)} J_1 + K_{11}^{(2)} J_2 \right) \quad (53)$$

where

$$J_1 = \int_0^H [(B' - b)s]^2 ds \quad (54)$$

$$J_1 = \int_0^H (B' - b)^2 s^2 ds = \frac{(B' - b)^2}{3} s^3 \Big|_0^H$$

$$\boxed{J_1 = \frac{(B' - b)^2}{3} H^3} \quad (55)$$

and

$$J_2 = \int_H^{b+H} [(B' - H)s - bH]^2 ds \quad (56)$$

$$\begin{aligned} J_2 &= \int_H^{b+H} [(B' - H)^2 s^2 - 2(B' - H)bHs + b^2 H^2] ds \\ &= \left[\frac{(B' - H)^2}{3} s^3 - (B' - H)bHs^2 + b^2 H^2 s \right] \Big|_H^{b+H} \end{aligned}$$

so

$$J_2 = \frac{(B' - H)^2}{3} \left[(H+b)^3 - H^3 \right] - (B' - H)bH \left[(b+H)^2 - H^2 \right] + b^3 H^2$$

or

$$J_2 = \frac{(B'-H)^2}{3} [(H+b)^3 - H^3] - (B'-H)bH[(b+H)^2 - H^2] + b^3H^2 \quad (57)$$

If

$$K_{11}^{(1)} = K_{11}^{(2)} = K \quad (58)$$

then

$$C_{77}^R = 4K_{11}(J_1 + J_2) \quad (59)$$

AN APPLICATION

In our case, the parameters are

$$L' = 0.5265 \quad ; \quad H = 0.1469 \quad ; \quad L = 0.6210 \quad ; \quad R = 1.3861 \quad [\text{IN}]$$

then the enclosed area, A_e , and the circumference, c , of D spar are

$$A_e = 0.2776 \quad [\text{IN}^2] \quad ; \quad c = 2.6345 \quad [\text{IN}]$$

therefore

$$B = 0.2107 \quad [\text{IN}]$$

For $[+20, -70, +20, -70, -70, +20]$ Graphite / Epoxy

$$K_{11} = 0.3139 \text{ E}6$$

and

$$C_{77} = 0.06645 \text{ E}5 \quad [\text{lb-in}^4]$$

Using the equivalent rectangular area approach

$$H = 0.1469 \quad ; \quad b = 0.4724 \quad [\text{IN}]$$

and

$$A_e = 0.2776 \quad [\text{IN}^2] \quad ; \quad c = 2.4772 \quad [\text{IN}]$$

so

$$B' = 0.2241 \quad [\text{IN}]$$

and

$$C_{77}^R = 0.05964 \text{ E}5 \quad [\text{lb-in}^4]$$

The error produced between C_{77} and C_{77}^R is $\sim 10.3\%$ but, for instance twist tip deflection due to applied torque case the error produced is $\sim 0.3\%$.

ANALYSIS, DESIGN AND ELASTIC TAILORING
OF COMPOSITE ROTOR BLADES

Lawrence W. Rehfield and Ali R. Atilgan
Center for Rotary Wing Aircraft Technology
Georgia Institute of Technology
Atlanta, Georgia 30332



Final Report
Grant No. NAG-1-638
September 1987

PREFACE

This report summarizes the development of structural models for composite rotor blades. The models are intended for use in design analysis for the purpose of exploring the potential of elastic tailoring. The research has been performed at the Center for Rotary Wing Aircraft Technology, Georgia Institute of Technology. Professor Lawrence W. Rehfield was the Principal Investigator.

Close collaboration with Mark Nixon, Renee Lake, Gary Farley and Wayne Mantay of the Army Aerostructures Directorate, Langley Research Center, was maintained throughout the investigation.

INTRODUCTION

Composite material systems are now the primary materials for helicopter rotor system applications. In addition to reduced weight and increased fatigue life, these materials provide designs with fewer parts which means increased service life and improved maintainability. Also, in terms of manufacturing, it is possible to achieve more general aerodynamic shapes including flapwise variation in planform, section and thickness.

The aeroelastic environment in which rotor blades operate consists of inertial, aerodynamic and elastic loadings. Because of the directional nature of the composite materials, it is possible to construct rotor blades with different ply orientations and hybrid combinations of materials exhibiting coupling between various elastic modes of deformation. For example, if the fibers are placed asymmetrically in the upper and lower portions of the blade, there will be a twist induced by flapwise bending. This provides a potential for improving the performance of a lifting surface through aeroelastic tailoring of the primary load-bearing structure. Aeroelastic tailoring of a composite structure involves a design process in which the materials and dimensions are selected to yield specific coupling characteristics which in turn enhance the overall performance of the structure. The design of such advanced structures requires simple and reliable analytical tools which can take into consideration the directional nature of these materials. In this report, a description of analytical models is presented which aid in the design of composite rotor blades.

SUMMARY OF ACCOMPLISHMENTS

Foundation Provided by Previous Work

The present research had its origin in the development and application of a new structural model for composite rotor blades with a single structural cell. The theory is presented in Accomplishment 1, an extensive numerical comparative study appears in Accomplishment 2 and a comparison with box beam experiments is given in Accomplishment 3. This body of knowledge established a sound technology base for applications and design-related studies.

Research Objectives

The present work has three main purposes. They are

1. Support the research underway at the Aerostructures Directorate;
2. Develop simple analytic solutions for beam vibrations for comparison with tests and finite element simulations; and
3. Develop, validate and complete a simple analysis approach for multicell beams.

Item 1 has lead to Accomplishments 5-9 and 13. Item 3 corresponds to Accomplishment 11. Work supporting item 2 was presented in an informal report to the Langley Research Center.

Single Cell Theory

The theory of Rehfield¹ was compared with a finite element simulation of the static response of a model rotor blade². While the results showed generally good agreement, the effect of torsion-related warping was not accounted for. Later a complete analysis was performed⁵ which provided excellent agreement. Also, a physical assessment of the various elastic couplings has been made.

A summary of the above results appears in Appendix I, which is the abstract corresponding to Accomplishment 13. Also, a description of the improvements in twisting kinematics over the original theory¹ is provided.

Multicell Theory

Multicell theory requires a new modeling approach. The essential difference between single cell and multicell thin-walled beams is in the analysis of torsion. The innovative approach that has been used¹¹ is described in Appendix II. This appendix is the abstract for a new paper that has been submitted for presentation at the 29th AIAA SDM Conference.

ACCOMPLISHMENTS

Publications

1. Rehfield, L.W., "Design Analysis Methodology for Composite Rotor Blades," Proceedings of the Seventh DoD/NASA Conference on Fibrous Composites in Structural Design, AFWAL-TR-85-3094, June 1985, pp. (V(a)-1)-(V(a)-15).
2. Hodges, R.V., Nixon, M.W. and Rehfield, L.W., "Comparison of Composite Rotor Blade Models: Beam Analysis and an MSC Nastran Shell Element Model," NASA Technical Memorandum 89024, January 1987.
3. Bauchau, O., Coffenberry, B.S. and Rehfield, L.W., "Composite Box Beam Analysis: Theory and Experiments," Journal of Reinforced Plastics and Composites, Vol. 6, January 1987, pp. 25-35.

Presentations

4. Rehfield, L.W., "Design Issues for Modern Helicopter Rotor System Structures," Memorial Lecture to Honor James Alvin Stricklin, Texas A&M University, College Station, TX, 22 May 1986.
5. Rehfield, L.W., "Some Observations on the Behavior of the Langley Model Rotor Blade," U.S.A. Aerostructure Directorate, Langley Research Center, Hampton, VA, 24 July 1986.
- 6-9. Rehfield, L.W., "Structural Technology for Elastic Tailoring of Rotor Blades," presented at:
 - Army Research Office, Durham, NC, 25 September 1986.
 - USA Aeroflightdynamics Directorate, Ames Research Center, Moffett Field, CA, 29 September 1986.
 - University of Texas, Arlington, TX, 3 March 1987
 - Bell Helicopter Textron, Inc., Ft. Worth, TX, 4 March 1987
10. Hodges, D.H., and Rehfield, L.W., "Effect of Composite Blade Elastic Couplings on Stability," U.S.A. Aerostructures Directorate, Langley Research Center, Hampton, VA, 12 November 1986.
11. Rehfield, L.W. and Atilgan, Ali R., "Analysis of Multicell Thin-Walled Composite Beam Structures," U.S.A. Aerostructures Directorate, Langley Research Center, VA, 12 November 1986.
12. Rehfield, L.W., "An Overview of Composite Rotor System Research," The Ohio State University, Columbus, OH, 14 January 1987.
13. Rehfield, L.W. and Atilgan, A.R., "A Structural Model for Composite Rotor Blades and Lifting Surfaces," Paper AIAA-87-0769-CP, 28th SDM Conference, Monterey, CA, 6-8 April 1987.
14. Rehfield, L.W., "New Developments in Composite Rotor System Structures," University of California, Davis, CA, 21 May 1987.

APPENDIX I
SINGLE CELL THEORY

A STRUCTURAL MODEL FOR COMPOSITE
ROTOR BLADES AND LIFTING SURFACES*

Lawrence W. Rehfield and Ali R. Atilgan**
Center for Rotary Wing Aircraft Technology
School of Aerospace Engineering
Georgia Institute of Technology
Atlanta, Georgia 30332
(404)894-3067

EXTENDED ABSTRACT

Introduction

Composite material systems are currently primary candidates for aerospace structures. One key reason for this is the design flexibility that they offer. It is possible to tailor the material and manufacturing approach to the application. Two notable examples are the wing of the Grumman/USAF/DARPA X-29 and rotor blades under development by the U.S.A. Aerostructures Directorate (AVSCOM), Langley Research Center.¹

A working definition of elastic or structural tailoring is the use of structural concept, fiber orientation, ply stacking sequence and a blend of materials to achieve specific performance goals. In the design process, choices of materials and dimensions are made which produce specific response characteristics which permit the selected goals to be achieved. Common choices for tailoring goals are preventing instabilities or vibration resonances or enhancing damage tolerance.

* Sponsored by ARO under Contract DAAS29-82-K-0097 and by USA Aerostructures Directorate under grant NAG1-638.

** Professor, Associate Fellow AIAA and NATO Scholar, respectively.

An essential, enabling factor in the design of tailored composite structures is structural modeling that accurately, but simply, characterizes response. Simplicity is needed as cause-effect relationships between configuration and response must be clearly understood and numerous design iterations are required. The objective of this paper is to improve the single closed-cell beam model previously developed by the senior author² for composite rotor blades or lifting surfaces and to demonstrate its usefulness in applications.

Modeling Improvements

Two major improvements have been made in the model of Reference 2. They are:

- (1) More accurate representation of twisting deformation; and
- (2) Simplification of the representation of torsion-related warping.

Outline of the Present Work

An analysis of the behavior of the model Langley rotor blade under three static load cases appears in Reference 1. The model rotor cross section is shown in Figure 1. The same three loading cases have been considered. The first case is bending due to lift and blade weight, the second is pure torque and the third is axial loading due to centrifugal force.

In Reference 1, a classical version of the theory of Reference 2 is compared with an extensive finite element simulation based upon orthotropic shell elements. Attention is focused upon the small discrepancies in the earlier study which are correctly

attributed to torsion-related warping. This confirms the findings reported in Reference 3. Also, an assessment of nonclassical effects in bending behavior has been made.

Bending Due to Lift and Blade Weight

Beam deflection results from the bending case appear in Figure 2. Bernouli-Euler, the classical engineering beam theory, results are denoted by "BE." This model is overly stiff. Also presented are three shear deformation models, SD1, SD2 and SD3, and the finite element results.

The shear deformation model S1 is an approximation obtained by setting the coupling stiffness C_{25} and C_{36} in Reference 2 to zero. This is the classical shear deformation model in the spirit of Timoshenko. Clearly it is overly stiff also. This direct transverse shear effect is small for a beam of this slenderness.

The complete theory, which includes all coupling effects, is denoted SD3. It provides good agreement with the finite element results.

The approximation denoted SD2 is obtained by neglecting completely the classical shear deformation effect accounted for in SD1 in favor of the coupling mechanism associated with C_{25} and C_{36} . This model, therefore, includes only deformations due to the transverse shear-bending coupling and the usual bending contribution. The magnitude of this new, unexplored form of elastic coupling is seen to be enormous by comparing SD2 and BE results. This is a finding of major importance in understanding the behavior.

The SD2 or SD3 models are required in this application in order to get sufficiently accurate predictions. This clearly excludes the earlier classical type theory of Mansfield and Sobey⁴ from practical use.

Pure Torque

The classical St. Venant torsion theory result (without warping) is compared to the complete beam theory (CBT) and the finite element results in Figure 3. The CBT results, which differ from the classical (CL) only by the warping effect, are in excellent agreement with the finite element analysis. Restrained warping creates a boundary layer zone near the blade root that acts to stiffen the blade and reduce the angle of twist.

Axial Loading Due to Centrifugal Force

This case is of the utmost importance because extension-twist coupling is to be used to control blade stall, an application of elastic tailoring. The discrepancy between analytical predictions and the finite element analysis was the greatest for this case. Classical theory was too soft and it overestimated the twist angle, a condition that is not conservative in view of the stated purpose of the model demonstration.

As in the pure torsion case, the neglect of torsion-related warping is the reason for the discrepancy between coupled beam theory and the finite element analysis.

The twist angle distribution appears in Figure 4. The use of CBT brings the beam theory results in very good agreement with the finite element analysis. The rate of twist distribution is given in Figure 5. Again, the agreement is very good.

Conclusions

In structures designed for extension-twist coupling, a high degree of bending-shear coupling is present which drastically causes the structure to be more flexible in bending. The impact of this effect on system performance must be assessed.

Torsion-related warping is significant enough to warrant its inclusion in the beam analysis. With warping accounted for, the coupled beam theory is extremely accurate and easy to use.

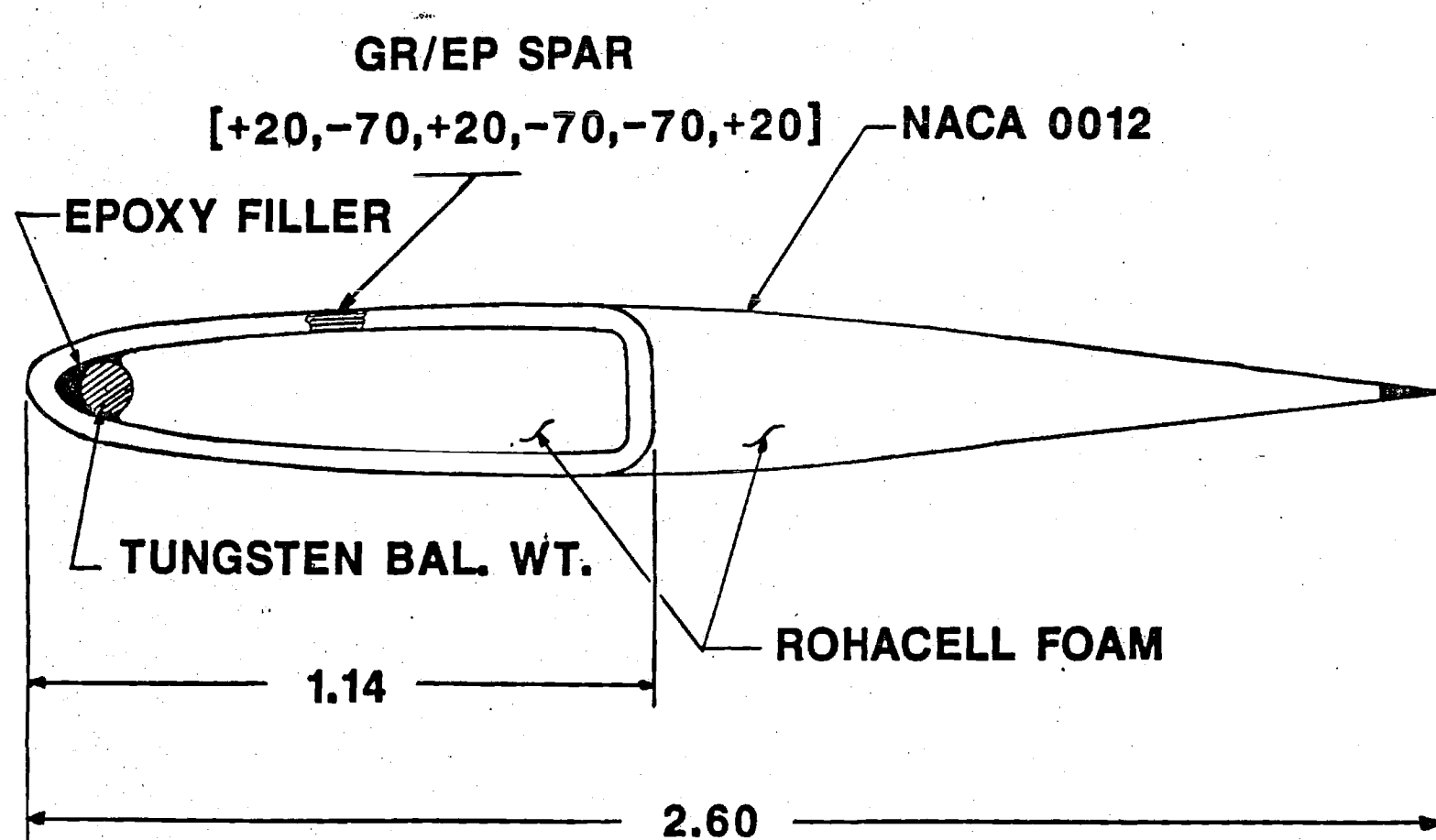
References

1. Hodges, R.V., Nixon, M.W. and Rehfield, L.W., "Comparison of Composite Rotor Blade Models: Beam Analysis and an MSC Nastran Shell Element Model," ARO Dynamics and Aeroelastic Stability Modeling Workshop, Georgia Institute of Technology, Atlanta, GA, 4-5 December 1985.

To be published as a NASA/AVSCOM Technical Memorandum, 1986.
2. Rehfield, L.W., "Design Analysis Methodology for Composite Rotor Blades," Proceedings of the Seventh DoD/NASA Conference on Fibrous Composites in Structural Design, AFWAL-TR-85-3094, June 1985, pp.(V(a)-1)-(V(a)-15).
3. Bauchau, O., Coffenberry, B.S. and Rehfield, L.W., "Composite Box Beam Analysis: Theory and Experiments," to appear in the January 1987 issue of the Journal of Reinforced Plastics and Composites.
4. Mansfield, E.H. and Sobey, A.J., "The Fibre Composite Helicopter Blade, Part 1: Stiffness Properties, Part 2: Prospect for Aeroelastic Tailoring," Aeronautical Quarterly, May 1979, pp. 413-449.

FIG. 1

MODEL ROTOR CROSS SECTION



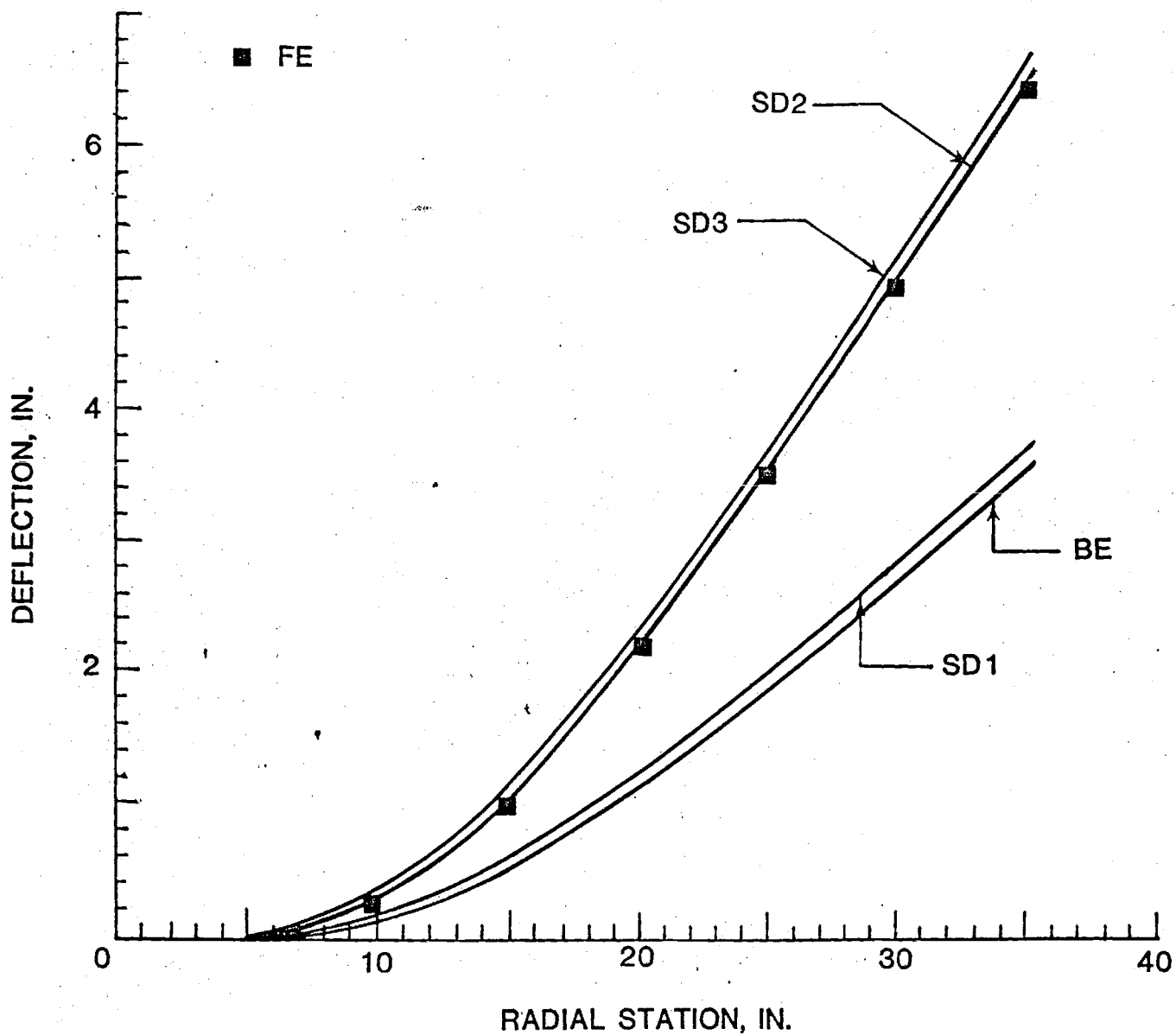


FIGURE 2
BEAM DEFLECTION DUE TO
LIFT AND BLADE WEIGHT

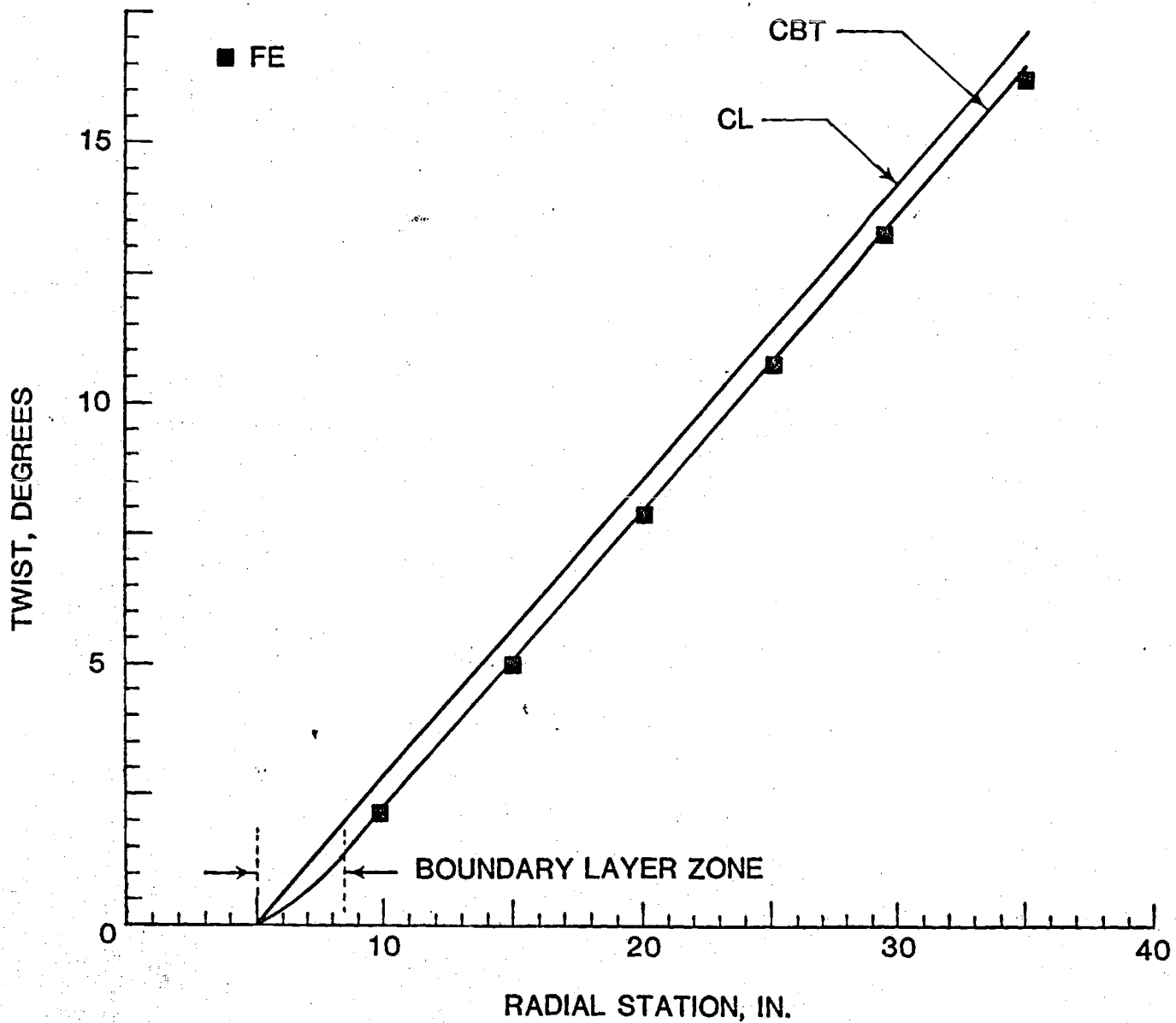


FIGURE 3

TWIST DUE TO APPLIED TORQUE

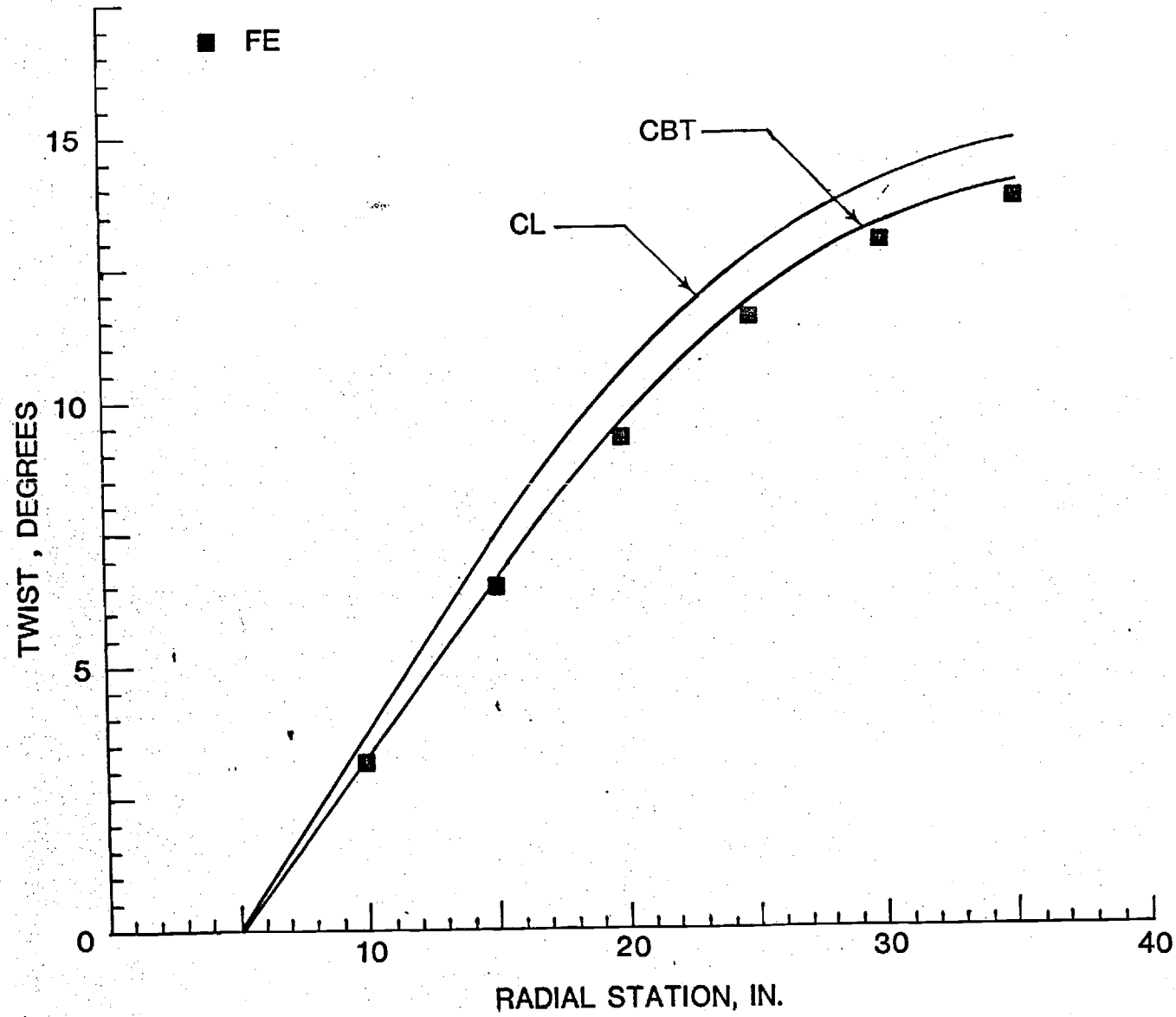


FIGURE 4
TWIST DUE TO CENTRIFUGAL FORCE

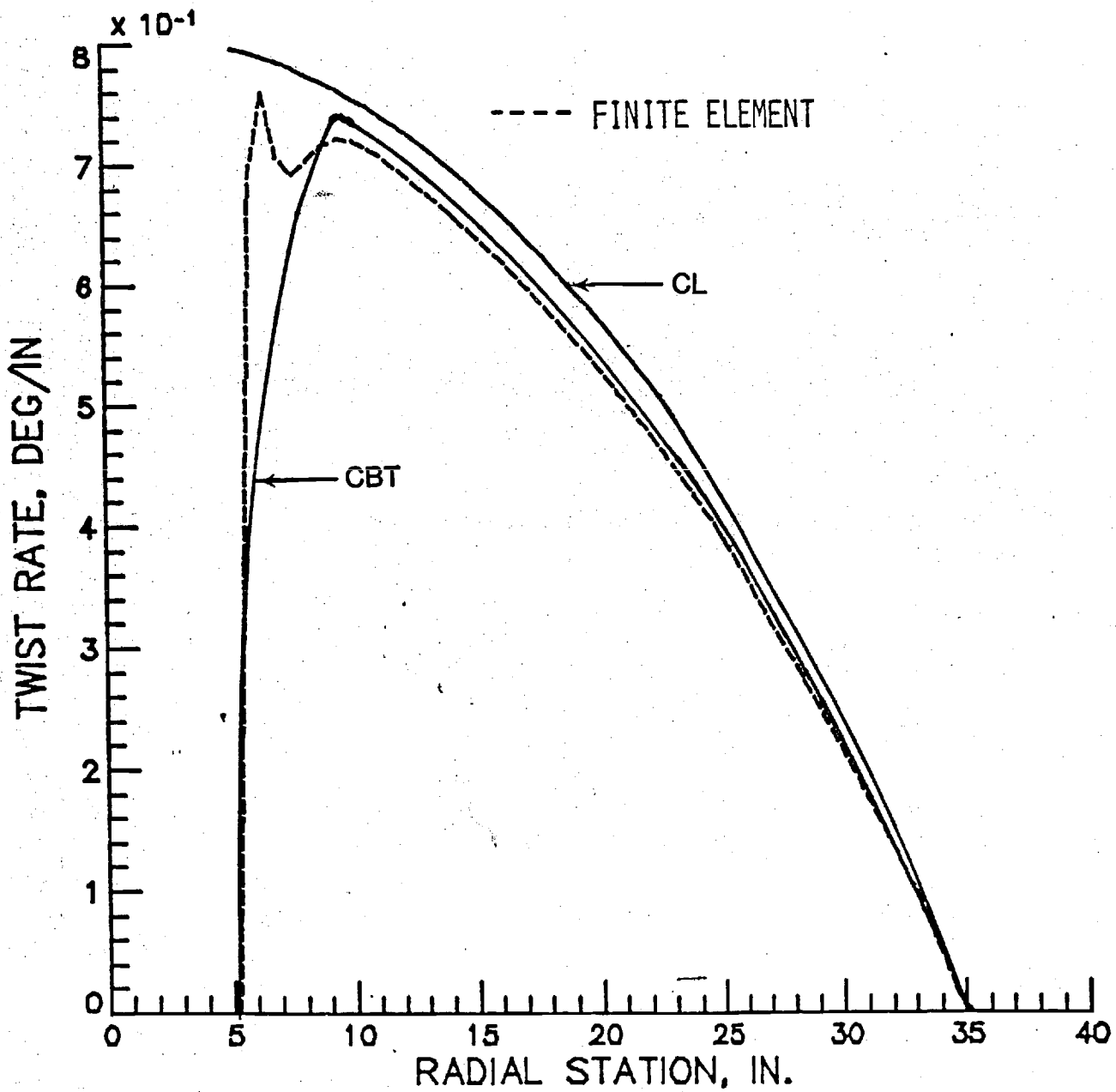


Figure 5. - Twist rate due to centrifugal force.

APPENDIX II
MULTICELL THEORY

STRUCTURAL MODELING FOR
MULTICELL COMPOSITE ROTOR BLADES

Lawrence W. Rehfield and Ali R. Atilgan**
Center for Rotary Wing Aircraft Technology
School of Aerospace Engineering
Georgia Institute of Technology
Atlanta, Georgia 30332
(404)894-3067

EXTENDED ABSTRACT

Introduction

Composite material systems are currently primary candidates for aerospace structures. One key reason for this is the design flexibility that they offer. It is possible to tailor the material and manufacturing approach to the application. Two notable examples are the wing of the Grumman/USAF/DARPA X-29 and rotor blades under development by the U.S.A. Aerostructures Directorate (AVSCOM), Langley Research Center.¹

A working definition of elastic or structural tailoring is the use of structural concept, fiber orientation, ply stacking sequence and a blend of materials to achieve specific performance goals. In the design process, choices of materials and dimensions are made which produce specific response characteristics which permit the selected goals to be achieved. Common choices for tailoring goals are preventing instabilities or vibration resonances or enhancing damage tolerance.

* Sponsored by ARO under Contract DAAS29-82-K-0097 and by USA Aerostructures Directorate under grant NAG1-638.

** Professor, Associate Fellow AIAA and NATO Scholar, respectively.

An essential, enabling factor in the design of tailored composite structures is structural modeling that accurately, but simply, characterizes response. Simplicity is needed as cause-effect relationships between configuration and response must be clearly understood and numerous design iterations are required. The objective of this paper is to present a new multicell beam model for composite rotor blades and to validate predictions based upon the new model by comparison with a finite element simulation in three benchmark static load cases.

Outline of the Present Work

The most significant difference between single cell and multicell thin-walled beams is in the analysis of torsion. The first step is to determine the shear center of the multicell section which is needed to establish the twisting kinematics. In the present approach, an innovative application of the unit load theorem is employed which utilizes the St. Venant torsion solution as a basis. This approach leads to closed form expressions for the coordinates of the shear center that are in terms of physically meaningful parameters.

Torsion-related warping, which earlier works^{2,3,4} on single cell theory indicate is important, is determined in a manner similar to that of Bescoter.⁵ In contrast to obtaining the stiffness matrix using the principle of virtual work², the unit load theorem is employed also to find the flexibility matrix, which is inverse of the stiffness matrix. Therefore, flexibilities are directly found, which is convenient for application.

After the above analytical steps are completed, the global beam theory is created in a manner similar to the single cell case.²

Application

The present model is applied to a two cell beam. The model cross section is shown in Figure 2. The benchmark static load cases appear in Figure 3. The first case is bending due to a tip load, the second is pure torque and the third is axial loading due to a centrifugal force.

The predictions are compared with an extensive finite element simulation⁶ based upon orthotropic shell elements. They are found to be in very good agreement as can be seen in Figures 4, 5 and 6.

Concluding Remarks

A multicell beam theory is developed and validated. Predictions based upon the new model are compared with an extensive finite element simulation as the means of validation.

References

1. Hodges, R.V., Nixon, M.W. and Rehfield, L.W., "Comparison of Composite Rotor Blade Models: Beam Analysis and an MSC Nastran Shell Element Model," NASA Technical Memorandum 89024, March 1987.
2. Rehfield, L.W., "Design Analysis Methodology for Composite Rotor Blades," Proceedings of the Seventh DoD/NASA Conference on Fibrous Composites in Structural Design, AFWAL-TR-85-3094, June 1985, pp.(V(a)-1)-(V(a)-15).
3. Bauchau, O., Coffenbery, B.S. and Rehfield, L.W., "Composite Box Beam Analysis: Theory and Experiments," Journal of Reinforced Plastics and Composites, Vol. 6, January 1987, pp. 25-35.

References (continued):

4. Rehfield, L.W. and Atilgan, A.R., "A Structural Model for Composite Rotor Blades and Lifting Surfaces," presented at 28th AIAA/ASME/AHS/ASCE Meeting, Monterey, California, 6-8 April 1987.
5. Bescoter, S.U., "A Theory of Torsion Bending for Multicell Beams," Journal of Applied Mechanics, March 1954, pp. 25-34.
6. Nixon, M.W., Private Communication, USA Aerostructures Directorate, Langley Research Center, Hampton, VA, June 1987.

[+ 20 , - 70 , + 20 , - 70 , - 70 , + 20]

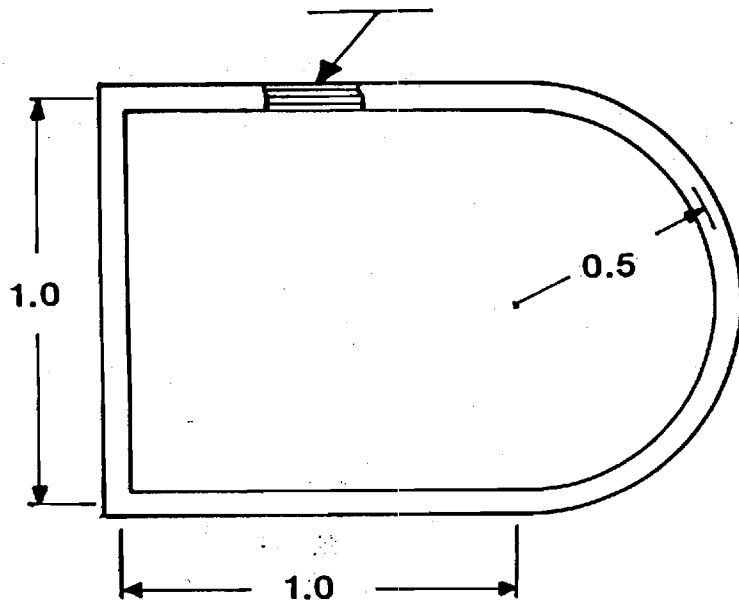


FIGURE 1. SINGLE CELL BEAM CROSS SECTION

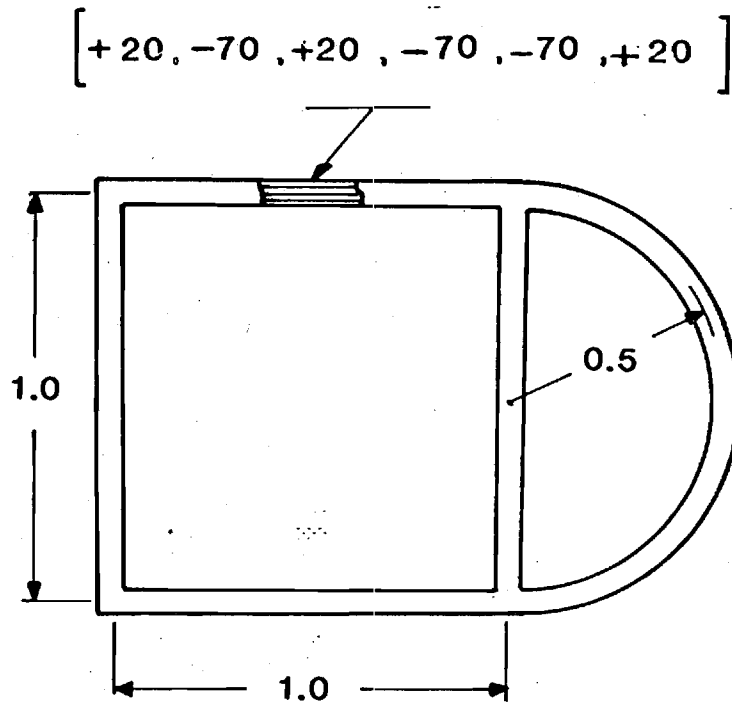
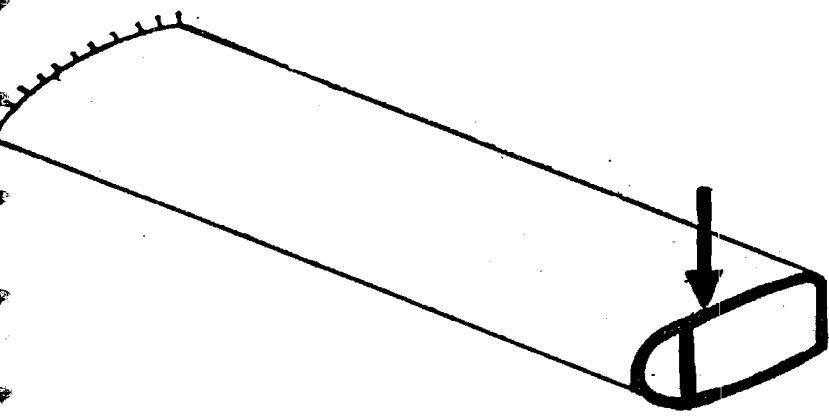
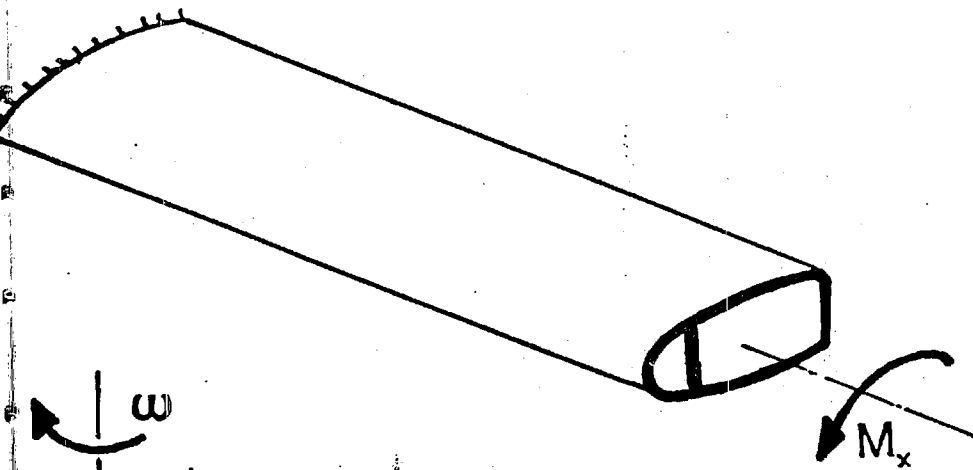


FIGURE 2. TWO CELL BEAM CROSS SECTION

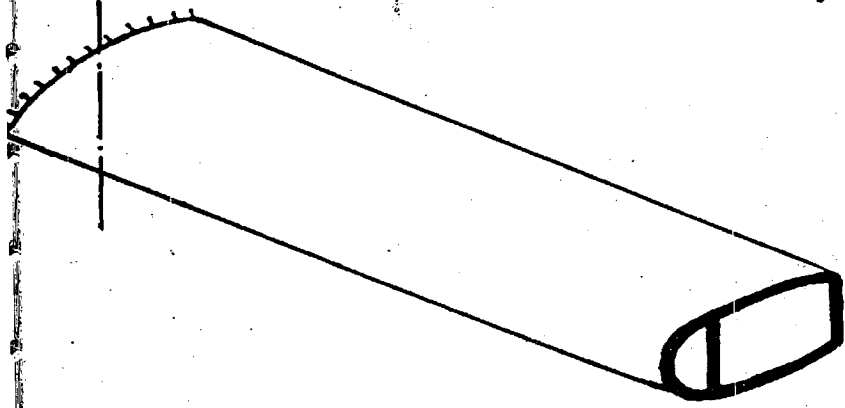
FIGURE 3. GENERIC STATIC LOAD CASES



TIP LOAD



PURE TORSION



CENTRIFUGAL LOADING

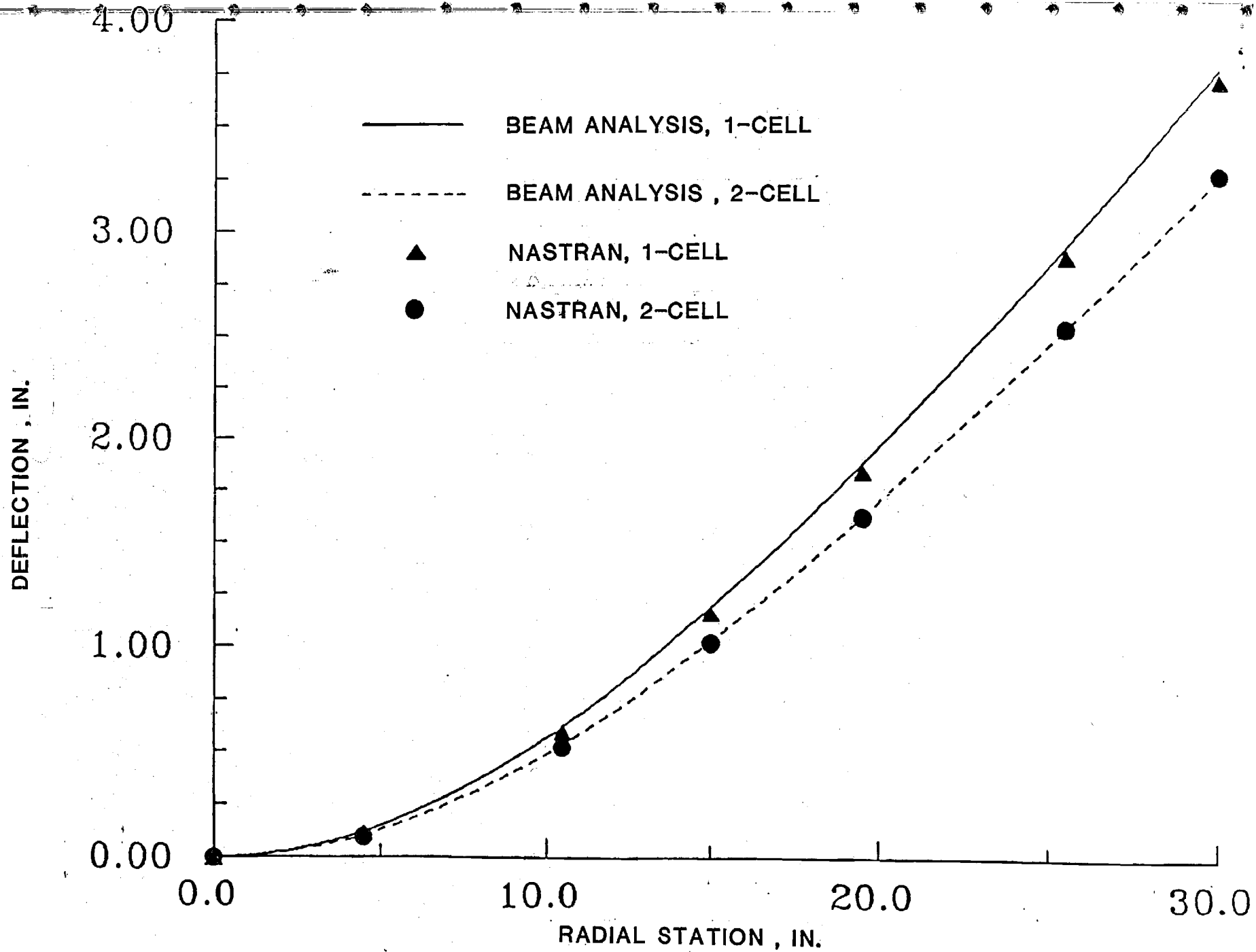


FIGURE 4. DEFLECTION DUE TO TIP LOAD

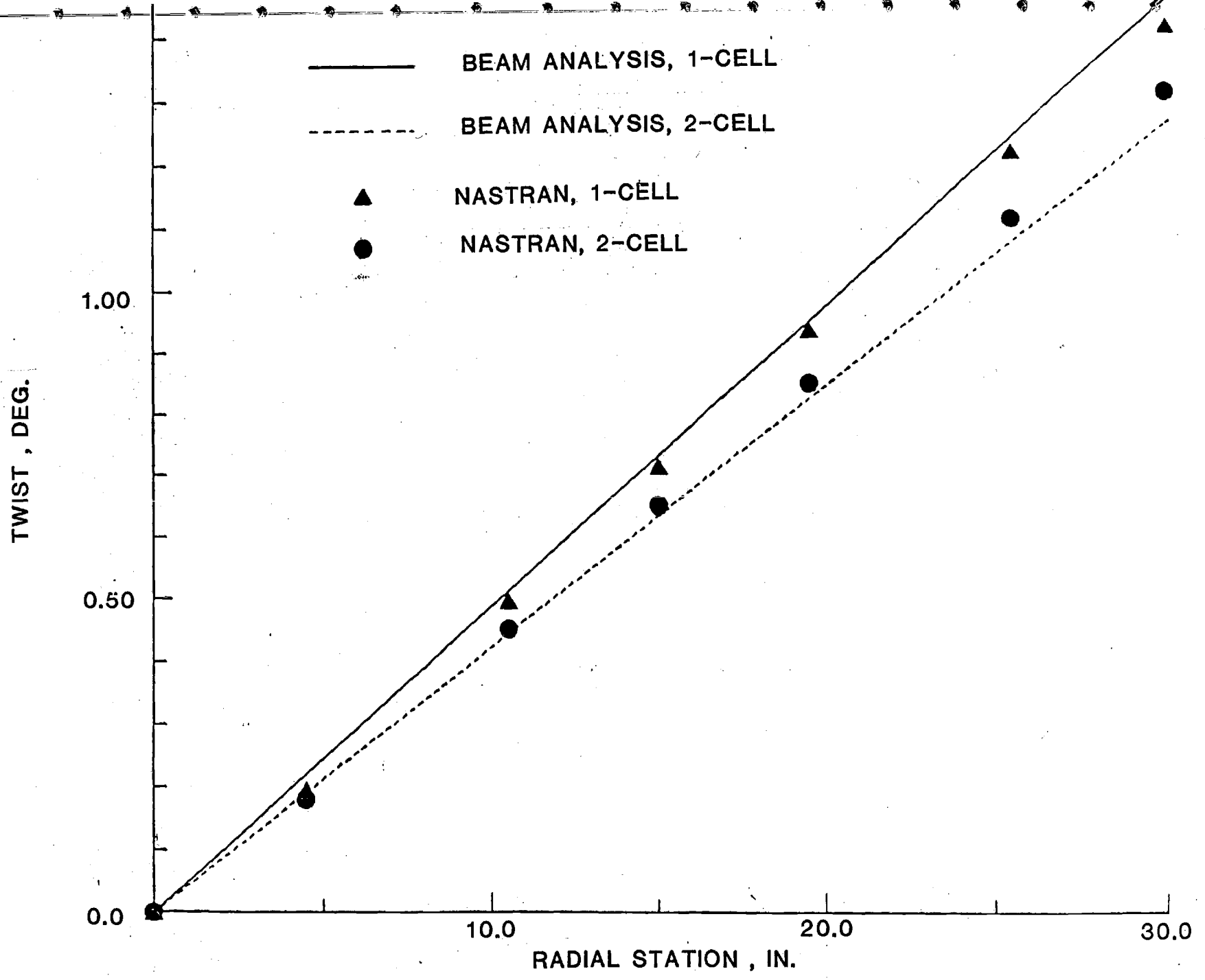


FIGURE 5. TWIST DUE TO PURE TORQUE

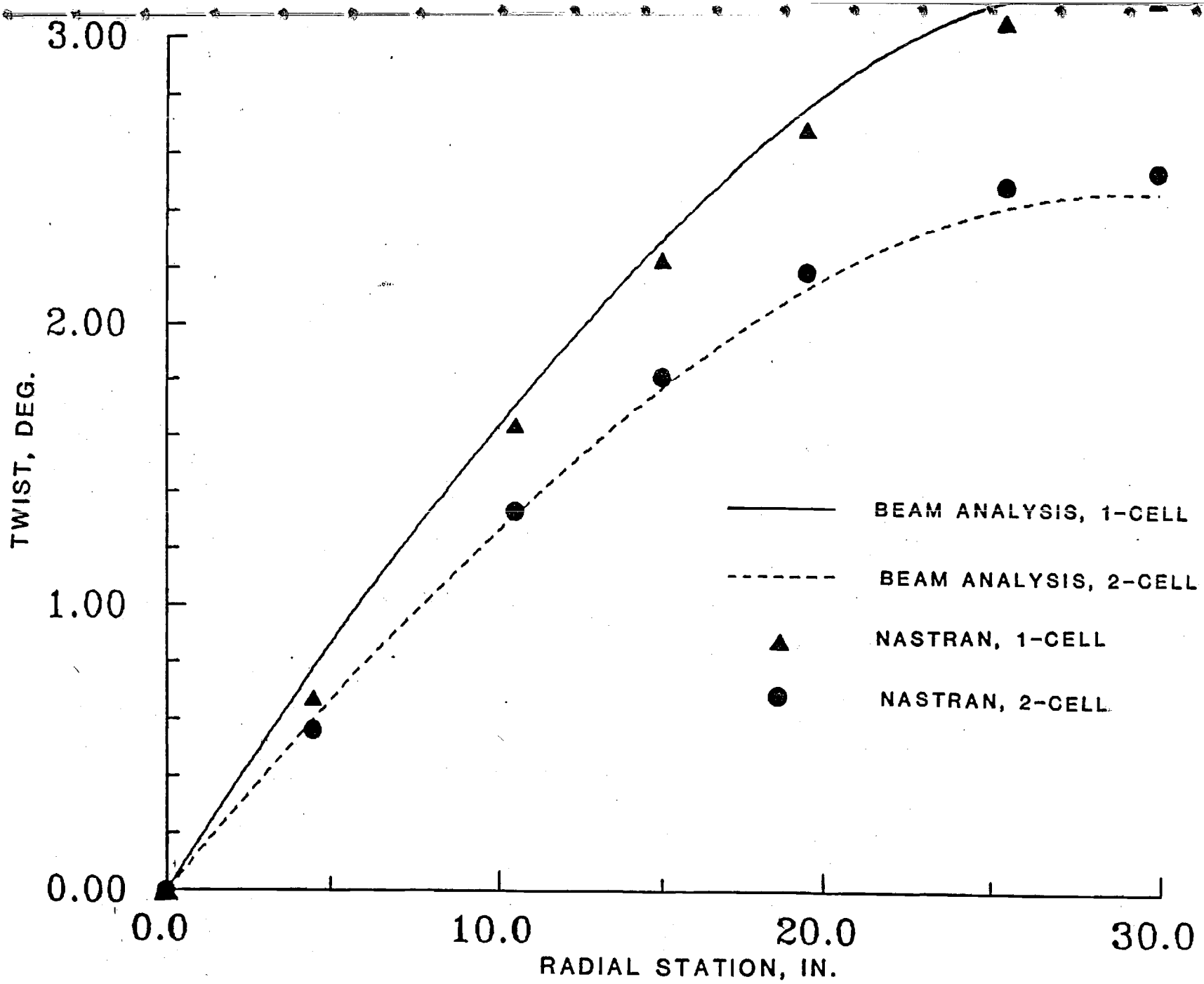


FIGURE 6. TWIST DUE TO CENTRIFUGAL FORCE